Selected Problems in the Mechanics of Natural and Artificial Small Bodies

Presented by Colby Merrill (They/Them)

July 30, 2024

Admission to Candidacy Examination

Outline

- [Natural] The ages of binary asteroids in equilibrium
- [Artificial] Thrust-enabled periodic trajectories in Cislunar space
- [Nat + Art] Binary asteroid mission designs

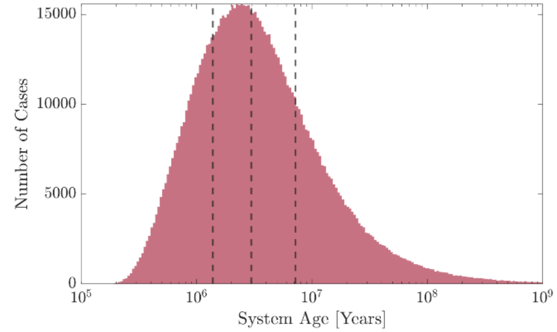

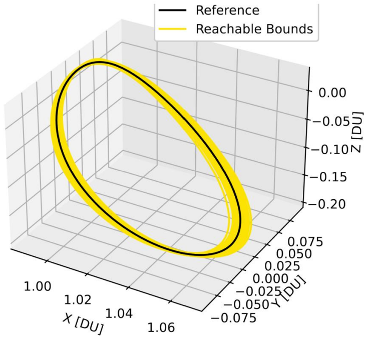

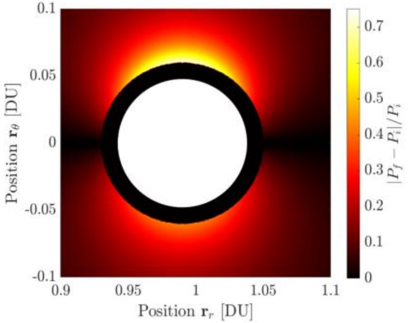

Topic 1: Binary Asteroid Equilibrium Ages

- 15% of asteroids have moons[1] formed via rotational fission[2]
- Absolute age data
  - Geologic history
  - Family formation
  - Physical properties
  - Dynamical history

[3, 4]

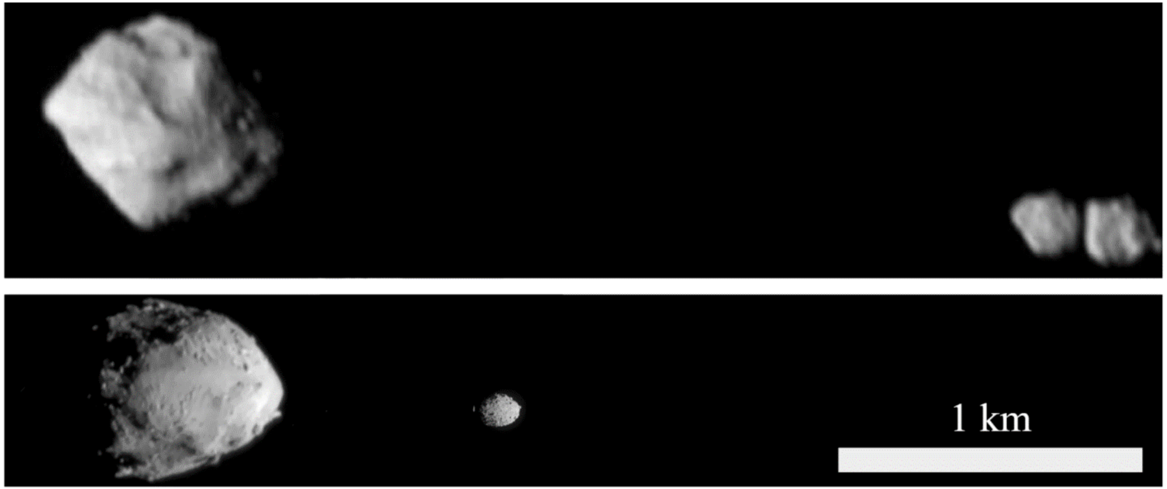

[1] Pravec et al., 2006, *Icarus*; [2] Walsh et al., 2008, *Nature*; [3] Chabot et al., 2024, *PSJ*; [4] Levison et al., 2024, *Nature*

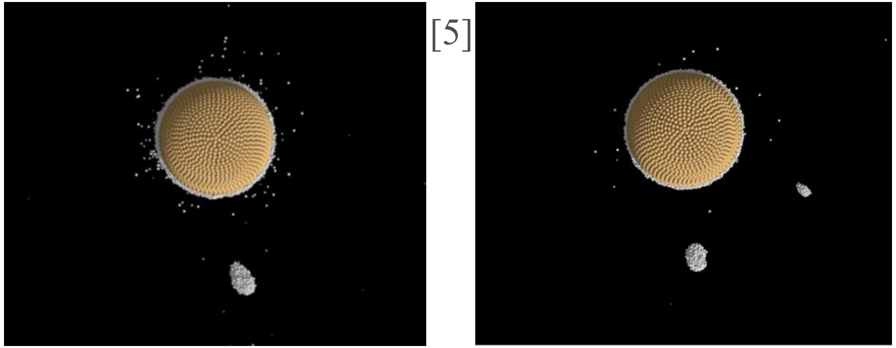

[5]

GOAL: How long does this process take?

[3, 4]

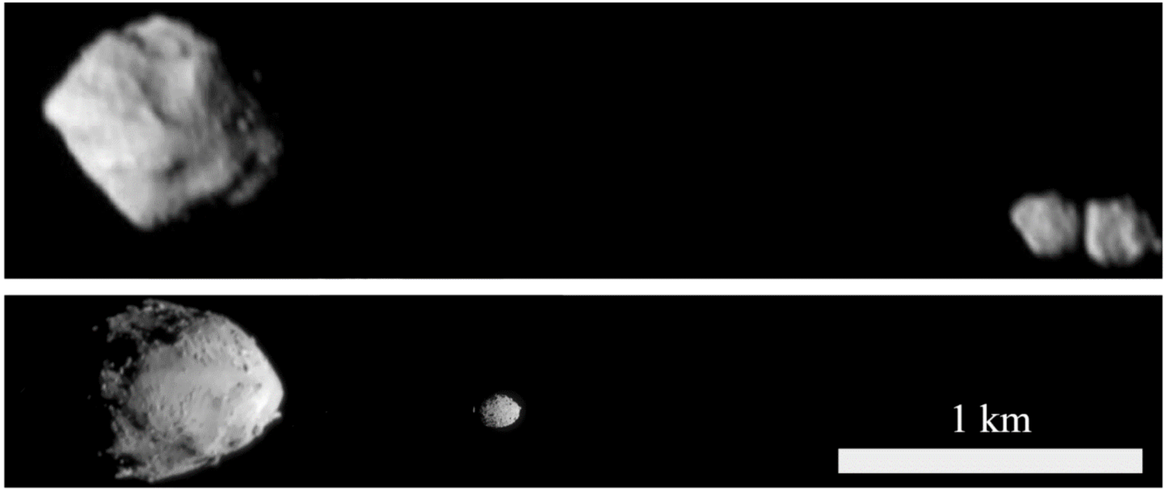

[3] Chabot et al., 2024, *PSJ*; [4] Levison et al., 2024, *Nature*; [5] Agrusa et al., 2024, *PSJ*

Method Assumptions

- Spin-fission conditions
  - Secondary at Roche limit
- *Nearly* in tidal-BYORP equilibrium
  - No eccentricity
  - Synchronous rotation
- Evolution dominated by tides, YORP, BYORP

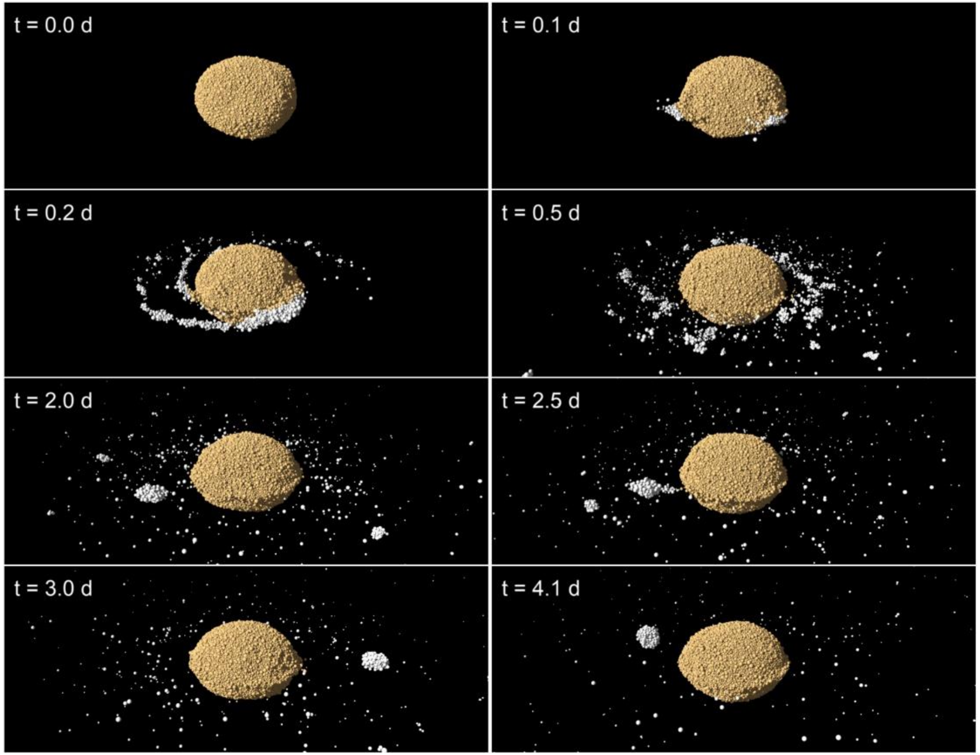

[5] Agrusa et al., 2024, *PSJ*

Tides, YORP, and BYORP

Tides shift angular momentum from primary to secondary

YORP + BYORP alter angular momentum

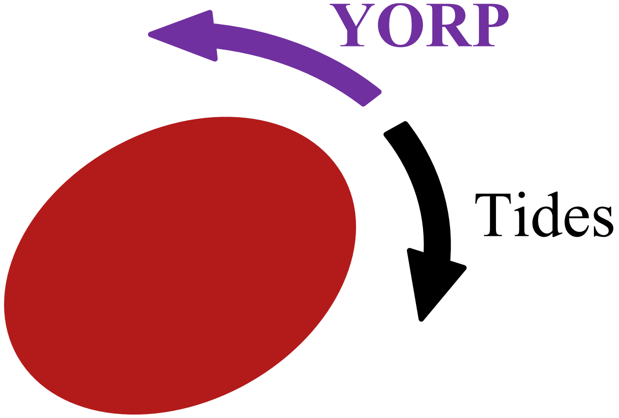

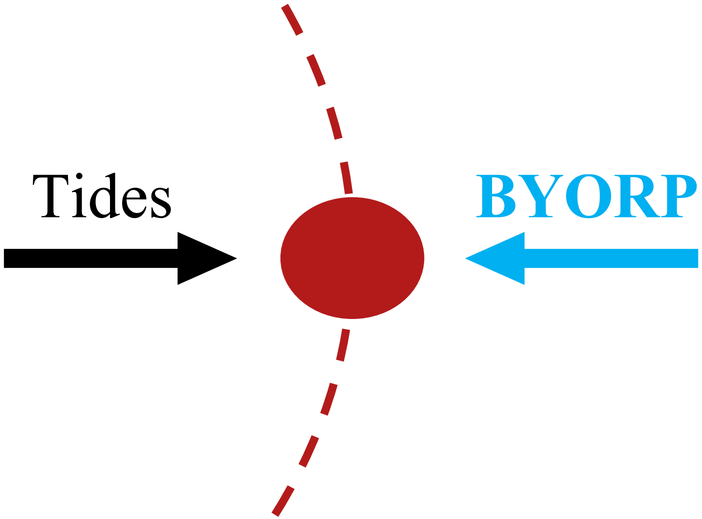

Changes to Secondary's Orbit

BYORP and tides [6, 7]

$$\dot{a}_B \propto a^{3/2} \boxed{B}$$

$$\dot{a}_T \propto \boxed{\frac{k}{Q}} \frac{1}{a^4}$$

When secondary is at a_{eq}, there is a **stable** equilibrium

$$a_{eq} \propto \left(\frac{k}{|B|Q} \right)^{1/7}$$

[6] McMahon and Scheeres, 2010, *Icarus*; [7] Murray and Dermott, 1999

Changes to Primary's Spin

YORP and tides[7, 8]

$$\dot{\omega}_{p,Y} \propto \boxed{C_Y} \qquad \dot{\omega}_{p,T} \propto \boxed{\frac{k}{Q}}\frac{1}{a^6}$$

When secondary is at a_Y, there is an equilibrium

$$a_Y \propto \left(\frac{k}{|C_Y|Q}\right)^{1/6}$$

[7] Murray and Dermott, 1999; [8] Rossi et al., 2009, *Icarus*

Monte Carlo Analysis: Dinkinesh + Selam

Group	Parameter	Variable type
Current system (final conditions)	Final mutual orbit period [h]	Fixed
	Eccentricity	Fixed
	Diameter of Dinkinesh [m]	Gaussian
	Diameter of Selam [m]	Gaussian
	a_{eq} [m]	Gaussian
Unknown parameters	k/Q	Log-Uniform
	Coefficient for YORP	Gaussian
	Coefficient for BYORP	Derived
	Density [$kg\,m^{-3}$]	Derived
Initial conditions	Initial primary spin [$rad\,s^{-1}$]	Derived
	Initial semi-major axis [m]	Uniform

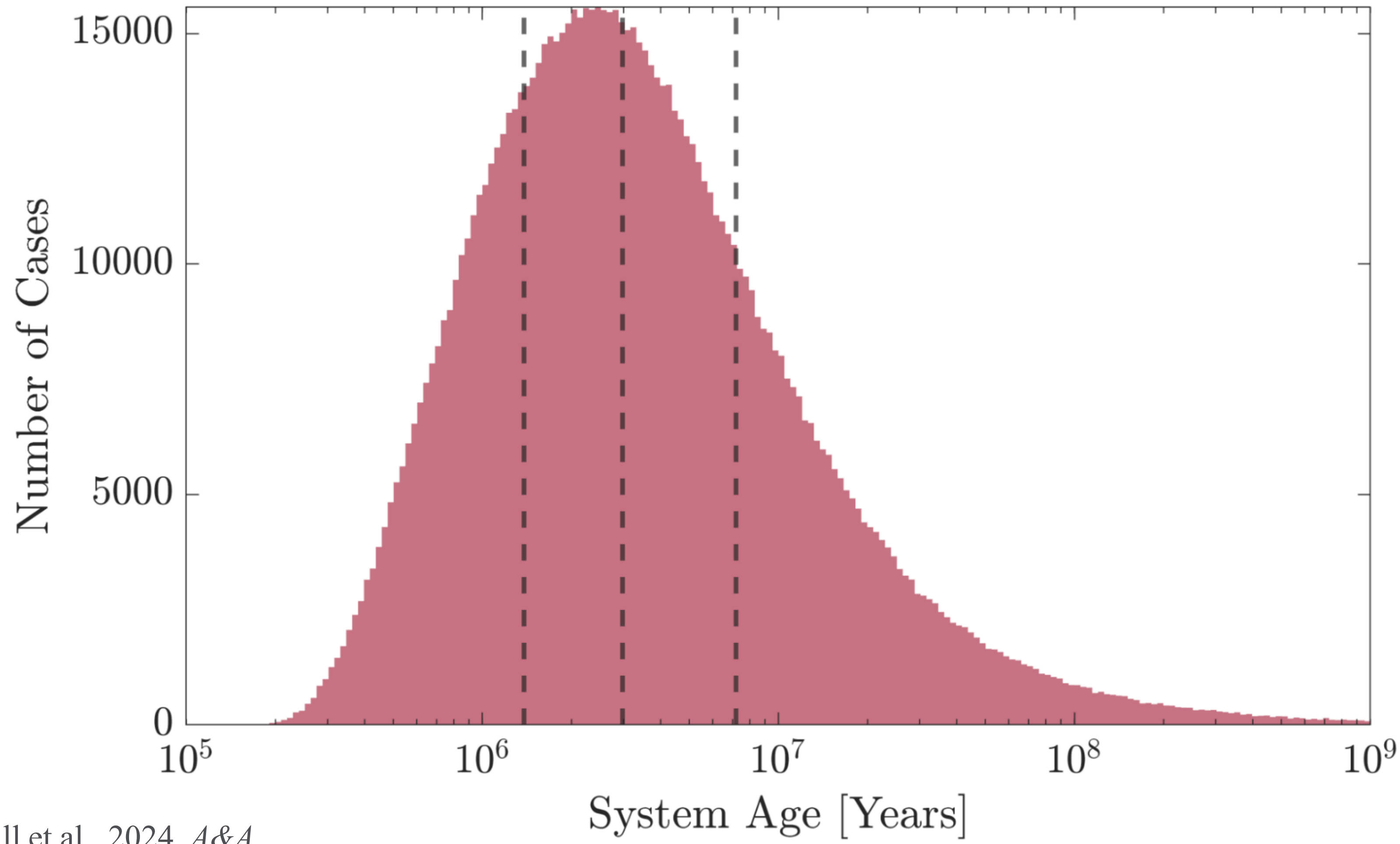

[9] Merrill et al., 2024, *A&A*

Pairing with Crater SFD

- Crater SFD indicates Selam's age = 2 Ma[10]
  - $k/Q > 6.0\text{e-}5$
  - $C_Y > -1.0\text{e-}2$
- Consistent with tidal-BYORP eq.
  - $|B|Q/k = 10.1 \pm 37\%$
  - $|B| > 6.1\text{e-}4 \pm 37\%$

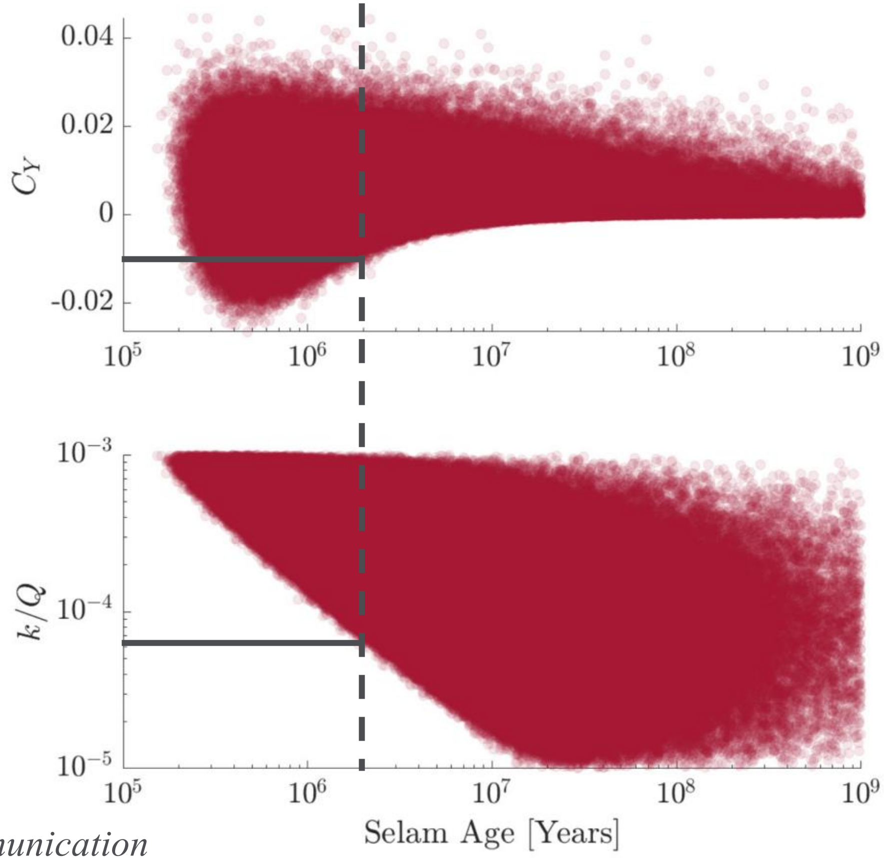

[9] Merrill et al., 2024, *A&A*; [10] Marchi, *personal communication*

Topic 1 Findings

- Selam's age is consistent with crater SFD
  - Evidence for BQ/k equilibrium for Dinkinesh
  - Constraints placed on k/Q, C_Y, B
- Improved condition for tidal-BYORP equilibrium
- New condition for tidal-YORP equilibrium

Topic 2: Energy-Optimal Periodic Trajectories

- Spacecraft often exploit periodic trajectories
- Very specific coverage of Cislunar space
- Thrust can expand this coverage
  - **By how much?**

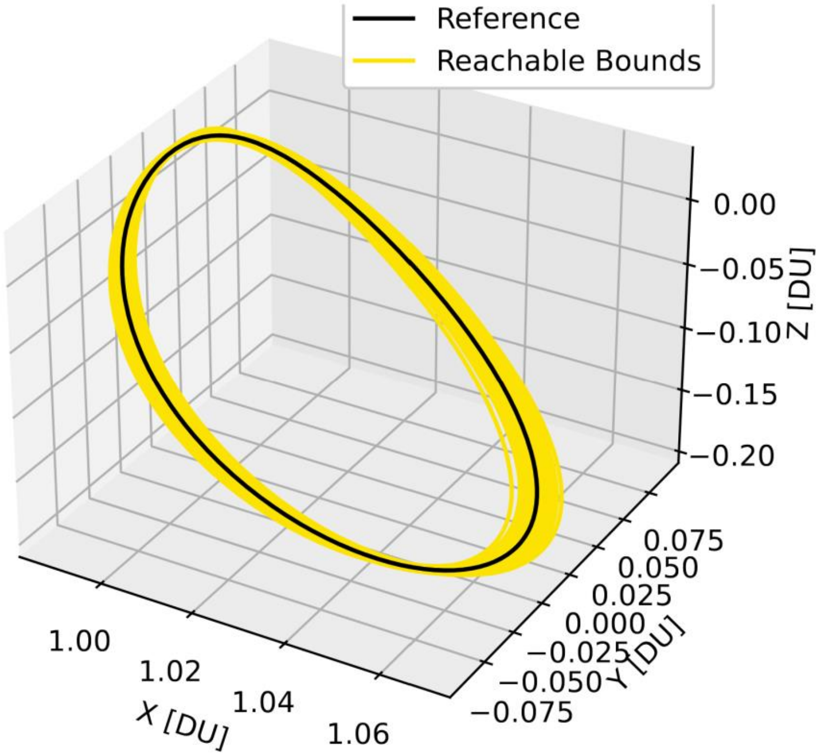

CR3BP (Synodic) Frame

- Assume circular orbits for m_1 and m_2
- Massless third body
- Rotating frame

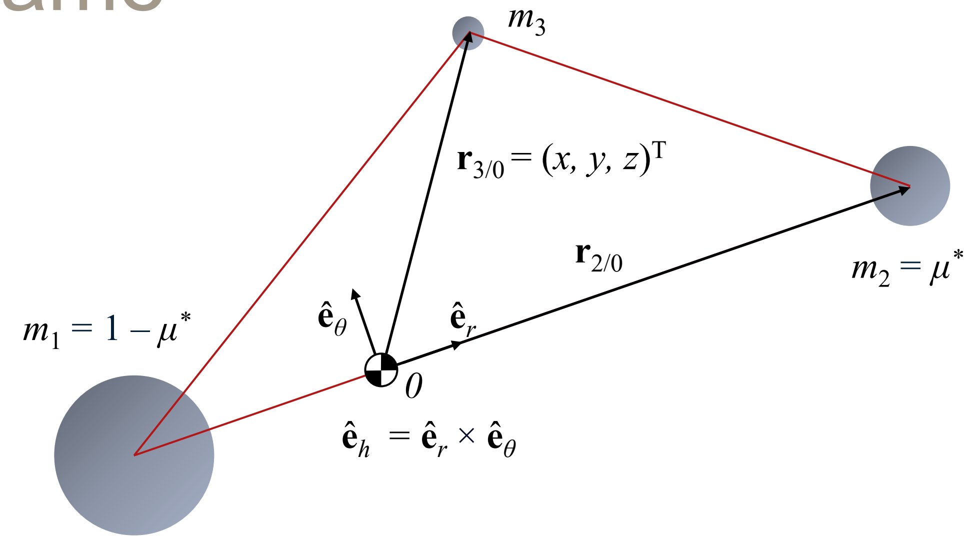

$$\mathbf{r} = \mathbf{r}_{3/0}$$

Optimization

- Optimality is achieved by finding the minimum value of J under control and constraints
  - Subject to constraints enforced by costates (e.g., λ_r and λ_v)
  - Meets boundary conditions (solves BVP)

Thrust

$$J = \frac{1}{2}\int_{t_0}^{t_f} ||\mathbf{u}||^2 dt$$

State

$$\mathbf{y} = \begin{bmatrix} \mathbf{x} \\ \boldsymbol{\lambda} \end{bmatrix} = \begin{bmatrix} \mathbf{r} \\ \mathbf{v} \\ \boldsymbol{\lambda}_r \\ \boldsymbol{\lambda}_v \end{bmatrix}$$

Costates

Augmented state

Roadmap: Solution to BVP

1. Define system of ODEs
   - Enforce constraints via Lagrange multipliers (costates)
2. Apply linear approximation
   - Introduce STMs
3. Solve for costates
4. Define cost as a function of state deviation and single matrix

$$J = \frac{1}{2}\int_{t_0}^{t_f} ||\mathbf{u}||^2 dt$$

↓

$$J = \frac{1}{2}\delta\mathbf{x}^T\mathbf{E}^*\delta\mathbf{x}$$

The system of ODEs:

CR3BP dynamics

Propagate the state (x) and costates (λ)

$$\begin{cases} \frac{\mathrm{d}\mathbf{x}}{\mathrm{d}t} = \mathbf{F}(\mathbf{x}) + \begin{bmatrix} 0_{3\times 1} \\ \mathbf{u} \end{bmatrix} \\ \frac{\mathrm{d}\boldsymbol{\lambda}}{\mathrm{d}t} = -\left(\frac{\partial \mathbf{F}(\mathbf{x})}{\partial \mathbf{x}}\right)^T \boldsymbol{\lambda} \end{cases}$$

Thrust (control)

$$\mathbf{u} = -\boldsymbol{\lambda}_v$$

$$J = \frac{1}{2}\int_{t_0}^{t_f} ||\mathbf{u}||^2 dt \quad \longrightarrow \quad J = \frac{1}{2}\int_{t_0}^{t_f} \boldsymbol{\lambda}_v^T \boldsymbol{\lambda}_v dt$$

Introducing a linear approximation

$$\delta \mathbf{y}(t_f) = \begin{bmatrix} \delta \mathbf{r}(t_f) \\ \delta \mathbf{v}(t_f) \\ \delta \boldsymbol{\lambda}_r(t_f) \\ \delta \boldsymbol{\lambda}_v(t_f) \end{bmatrix} \approx \underbrace{\begin{bmatrix} \boldsymbol{\Phi}_{\mathbf{r}}^{\mathbf{r}} & \boldsymbol{\Phi}_{\mathbf{v}}^{\mathbf{r}} & \boldsymbol{\Phi}_{\boldsymbol{\lambda}_r}^{\mathbf{r}} & \boldsymbol{\Phi}_{\boldsymbol{\lambda}_v}^{\mathbf{r}} \\ \boldsymbol{\Phi}_{\mathbf{r}}^{\mathbf{v}} & \boldsymbol{\Phi}_{\mathbf{v}}^{\mathbf{v}} & \boldsymbol{\Phi}_{\boldsymbol{\lambda}_r}^{\mathbf{v}} & \boldsymbol{\Phi}_{\boldsymbol{\lambda}_v}^{\mathbf{v}} \\ \boldsymbol{\Phi}_{\mathbf{r}}^{\boldsymbol{\lambda}_r} & \boldsymbol{\Phi}_{\mathbf{v}}^{\boldsymbol{\lambda}_r} & \boldsymbol{\Phi}_{\boldsymbol{\lambda}_r}^{\boldsymbol{\lambda}_r} & \boldsymbol{\Phi}_{\boldsymbol{\lambda}_v}^{\boldsymbol{\lambda}_r} \\ \boldsymbol{\Phi}_{\mathbf{r}}^{\boldsymbol{\lambda}_v} & \boldsymbol{\Phi}_{\mathbf{v}}^{\boldsymbol{\lambda}_v} & \boldsymbol{\Phi}_{\boldsymbol{\lambda}_r}^{\boldsymbol{\lambda}_v} & \boldsymbol{\Phi}_{\boldsymbol{\lambda}_v}^{\boldsymbol{\lambda}_v} \end{bmatrix}}_{\boldsymbol{\Phi}(t_f, t_0)} \delta \mathbf{y}_0$$

Final deviation to state

Initial deviation

STM

Notation for STMs

$$\boldsymbol{\Phi}_{\mathbf{a}}^{\mathbf{b}}(t, t_0) = \frac{\partial \mathbf{b}(t)}{\partial \mathbf{a}(t_0)}$$

Solve for $\delta\lambda_v$

$$\delta\mathbf{y}(t_f) = \begin{bmatrix} \delta\mathbf{r}(t_f) \\ \delta\mathbf{v}(t_f) \\ \delta\boldsymbol{\lambda}_r(t_f) \\ \delta\boldsymbol{\lambda}_v(t_f) \end{bmatrix} = \underbrace{\begin{bmatrix} \boldsymbol{\Phi}_{\mathbf{r}}^{\mathbf{r}} & \boldsymbol{\Phi}_{\mathbf{v}}^{\mathbf{r}} & \boldsymbol{\Phi}_{\boldsymbol{\lambda}_r}^{\mathbf{r}} & \boldsymbol{\Phi}_{\boldsymbol{\lambda}_v}^{\mathbf{r}} \\ \boldsymbol{\Phi}_{\mathbf{r}}^{\mathbf{v}} & \boldsymbol{\Phi}_{\mathbf{v}}^{\mathbf{v}} & \boldsymbol{\Phi}_{\boldsymbol{\lambda}_r}^{\mathbf{v}} & \boldsymbol{\Phi}_{\boldsymbol{\lambda}_v}^{\mathbf{v}} \\ \boldsymbol{\Phi}_{\mathbf{r}}^{\boldsymbol{\lambda}_r} & \boldsymbol{\Phi}_{\mathbf{v}}^{\boldsymbol{\lambda}_r} & \boldsymbol{\Phi}_{\boldsymbol{\lambda}_r}^{\boldsymbol{\lambda}_r} & \boldsymbol{\Phi}_{\boldsymbol{\lambda}_v}^{\boldsymbol{\lambda}_r} \\ \boldsymbol{\Phi}_{\mathbf{r}}^{\boldsymbol{\lambda}_v} & \boldsymbol{\Phi}_{\mathbf{v}}^{\boldsymbol{\lambda}_v} & \boldsymbol{\Phi}_{\boldsymbol{\lambda}_r}^{\boldsymbol{\lambda}_v} & \boldsymbol{\Phi}_{\boldsymbol{\lambda}_v}^{\boldsymbol{\lambda}_v} \end{bmatrix}}_{\boldsymbol{\Phi}(t_f, t_0)} \delta\mathbf{y}_0$$

$$\delta\boldsymbol{\lambda}_v(t) = \boldsymbol{\Phi}_{\mathbf{y}}^{\boldsymbol{\lambda}_v}(t, t_0)\delta\mathbf{y}_0 = \begin{bmatrix} \boldsymbol{\Phi}_{\mathbf{r}}^{\boldsymbol{\lambda}_v}(t, t_0) & \boldsymbol{\Phi}_{\mathbf{v}}^{\boldsymbol{\lambda}_v}(t, t_0) & \boldsymbol{\Phi}_{\boldsymbol{\lambda}_r}^{\boldsymbol{\lambda}_v}(t, t_0) & \boldsymbol{\Phi}_{\boldsymbol{\lambda}_v}^{\boldsymbol{\lambda}_v}(t, t_0) \end{bmatrix} \delta\mathbf{y}_0$$

Solve for J: ($\lambda_v = \delta\lambda_v$)

$$J = \frac{1}{2}\int_{t_0}^{t_f} \boldsymbol{\lambda}_v^T \boldsymbol{\lambda}_v dt \longrightarrow J = \frac{1}{2}\delta\mathbf{y}_0^T \left(\int_{t_0}^{t_f} \left(\boldsymbol{\Phi}_{\mathbf{y}}^{\boldsymbol{\lambda}_v}(t, t_0)\right)^T \left(\boldsymbol{\Phi}_{\mathbf{y}}^{\boldsymbol{\lambda}_v}(t, t_0)\right) dt \right) \delta\mathbf{y}_0$$

Explicitly solve the BVP

$$\delta \mathbf{y}_0 = \begin{bmatrix} \delta \mathbf{x}_0 \\ \delta \boldsymbol{\lambda}_0 \end{bmatrix} = \begin{bmatrix} \mathbf{I}_6 & \mathbf{0}_6 \\ -\left(\boldsymbol{\Phi}_{\boldsymbol{\lambda}}^{\mathbf{x}}\right)^{-1} \boldsymbol{\Phi}_{\mathbf{x}}^{\mathbf{x}} & \left(\boldsymbol{\Phi}_{\boldsymbol{\lambda}}^{\mathbf{x}}\right)^{-1} \end{bmatrix} \begin{bmatrix} \delta \mathbf{x}_0 \\ \delta \mathbf{x}_f \end{bmatrix}$$

Define a new matrix: $\mathbf{E}^*$

$$\mathbf{E} = \begin{bmatrix} \mathbf{I}_6 & \mathbf{0}_6 \\ -\left(\boldsymbol{\Phi}_{\boldsymbol{\lambda}}^{\mathbf{x}}\right)^{-1} \boldsymbol{\Phi}_{\mathbf{x}}^{\mathbf{x}} & \left(\boldsymbol{\Phi}_{\boldsymbol{\lambda}}^{\mathbf{x}}\right)^{-1} \end{bmatrix}^T \int_{t_0}^{t_f} \left(\boldsymbol{\Phi}_{\mathbf{y}}^{\boldsymbol{\lambda}_v}(t, t_0)\right)^T \left(\boldsymbol{\Phi}_{\mathbf{y}}^{\boldsymbol{\lambda}_v}(t, t_0)\right) dt \begin{bmatrix} \mathbf{I}_6 & \mathbf{0}_6 \\ -\left(\boldsymbol{\Phi}_{\boldsymbol{\lambda}}^{\mathbf{x}}\right)^{-1} \boldsymbol{\Phi}_{\mathbf{x}}^{\mathbf{x}} & \left(\boldsymbol{\Phi}_{\boldsymbol{\lambda}}^{\mathbf{x}}\right)^{-1} \end{bmatrix}$$

$$\mathbf{E}^* = \begin{bmatrix} \mathbf{I}_6 & \mathbf{I}_6 \end{bmatrix} \mathbf{E} \begin{bmatrix} \mathbf{I}_6 & \mathbf{I}_6 \end{bmatrix}^T$$

$$J = \frac{1}{2} \delta \mathbf{y}_0^T \left(\int_{t_0}^{t_f} \left(\boldsymbol{\Phi}_{\mathbf{y}}^{\boldsymbol{\lambda}_v}(t, t_0)\right)^T \left(\boldsymbol{\Phi}_{\mathbf{y}}^{\boldsymbol{\lambda}_v}(t, t_0)\right) dt \right) \delta \mathbf{y}_0 \longrightarrow J = \frac{1}{2} \delta \mathbf{x}^T \mathbf{E}^* \delta \mathbf{x}$$

Introducing a Thrust Constraint

- J is defined by the initial deviations in position and velocity and $\mathbf{E}^*$
- Maximum expended cost over one orbit = J^*
- Can now introduce the reachable set…

$$J = \frac{1}{2}\delta\mathbf{x}^T\mathbf{E}^*\delta\mathbf{x}$$

$$J^* = \frac{1}{2}u_{\max}^2(t_f - t_0)$$

The Reachable Set

[11]

semi-axis

$$\mathbf{a}_i = \sqrt{\frac{2J^*}{\gamma_i}}\mathbf{w}_i$$

eigenvector,
eigenvalue of $\mathbf{E}^*$

- Takes the form of a 6-D ellipsoid
- Mutually orthogonal semi-axes directions
- First semi-axis is not included in analysis

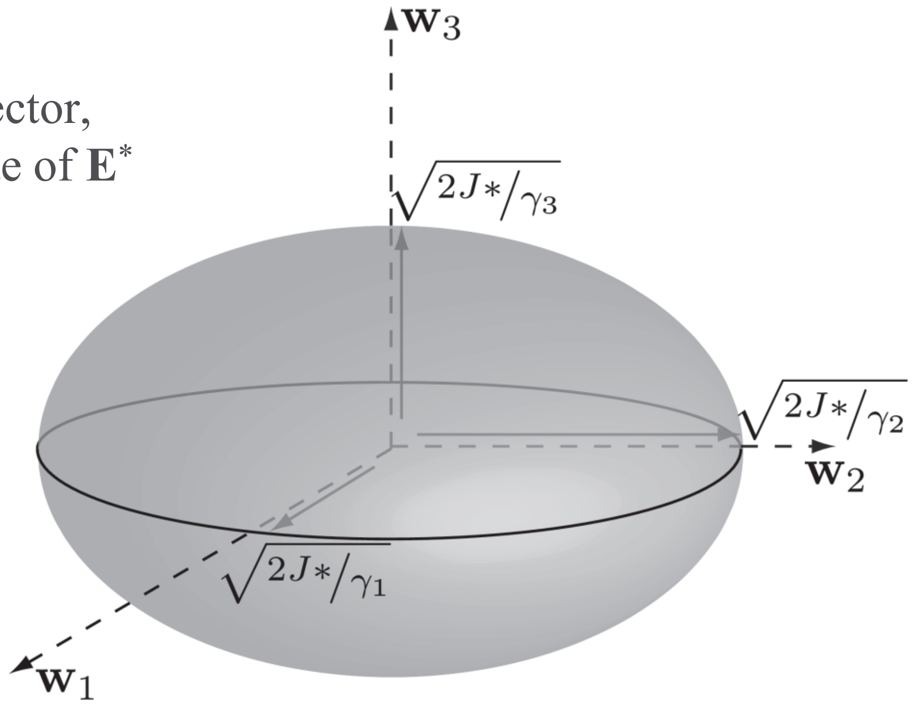

[11] Savransky, *personal communication*

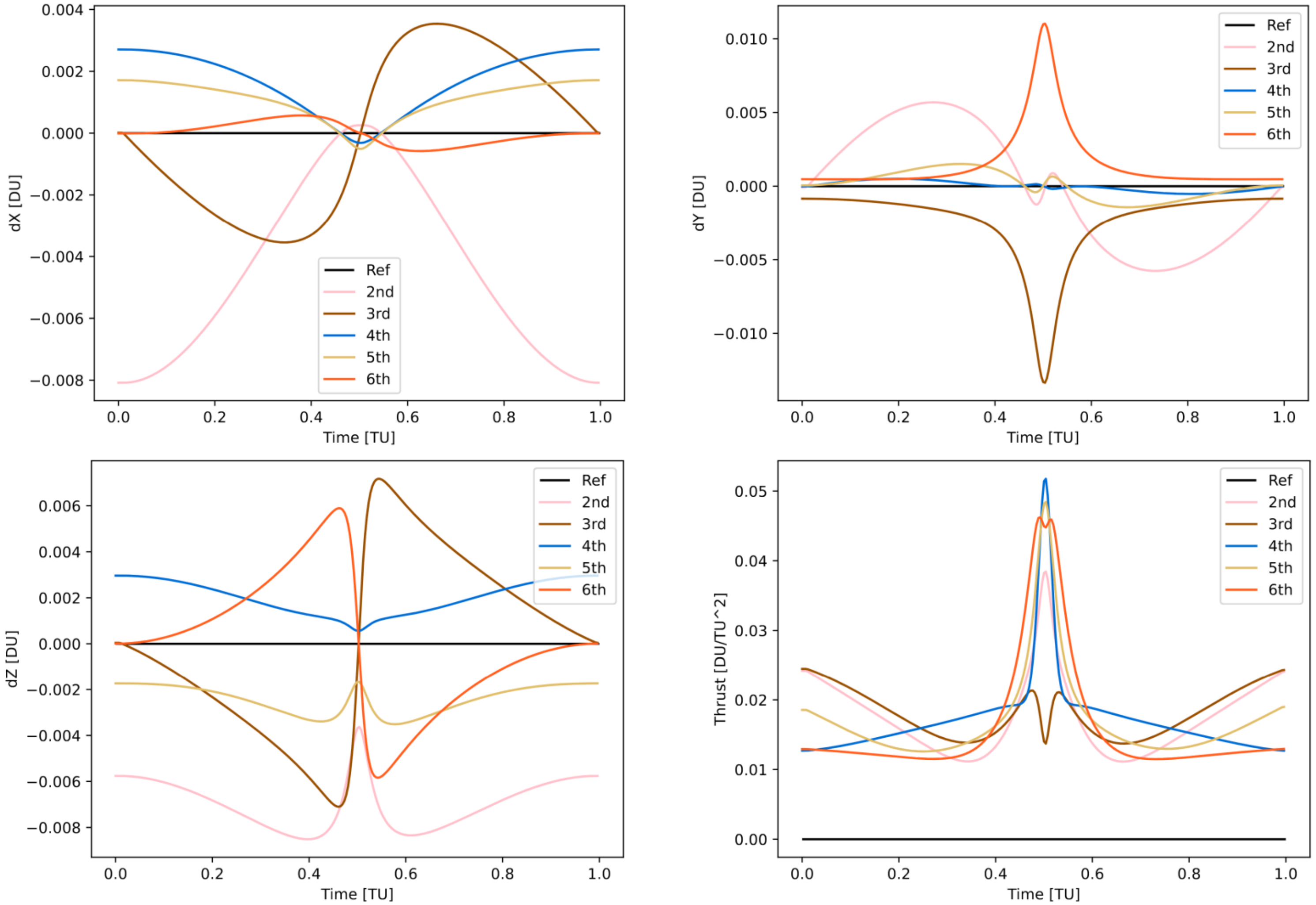
dX [DU]
Time [TU]
Ref
2nd
3rd
4th
5th
6th
dY [DU]
Time [TU]
Ref
2nd
3rd
4th
5th
6th
dZ [DU]
Time [TU]
Ref
2nd
3rd
4th
5th
6th
Thrust [DU/TU^2]
Time [TU]
Ref
2nd
3rd
4th
5th
6th

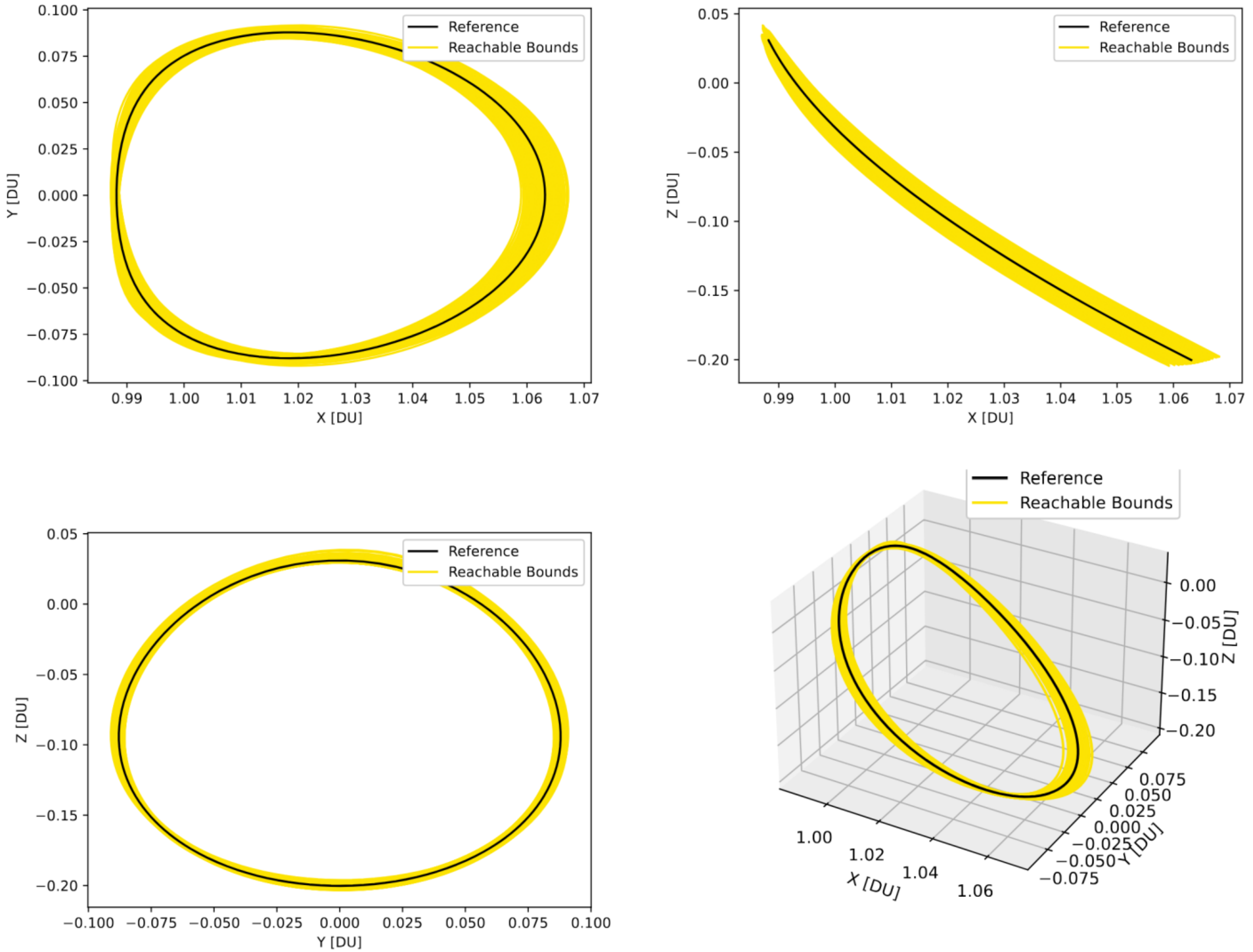

Reference
Reachable Bounds
X [DU]
Y [DU]
Z [DU]
0.99
1.00
1.01
1.02
1.03
1.04
1.05
1.06
1.07
0.100
0.075
0.050
0.025
0.000
−0.025
−0.050
−0.075
−0.100
0.05
0.00
−0.05
−0.10
−0.15
−0.20

Topic 2 Findings

- We have produced artificial periodic trajectories that were not known before
- Given J^*, the reachable set is a hyper-ellipsoid around a reference
- It is possible to reduce perilune distance (initial deviation along second eigenvector)

Topic 3: Binary Asteroid Mission Designs

- Models of evolution but no observed processes
  - Contact binary
  - Tidal disruption
  - Asteroid pair
- Spacecraft can reproduce binary evolution
- What is feasible?

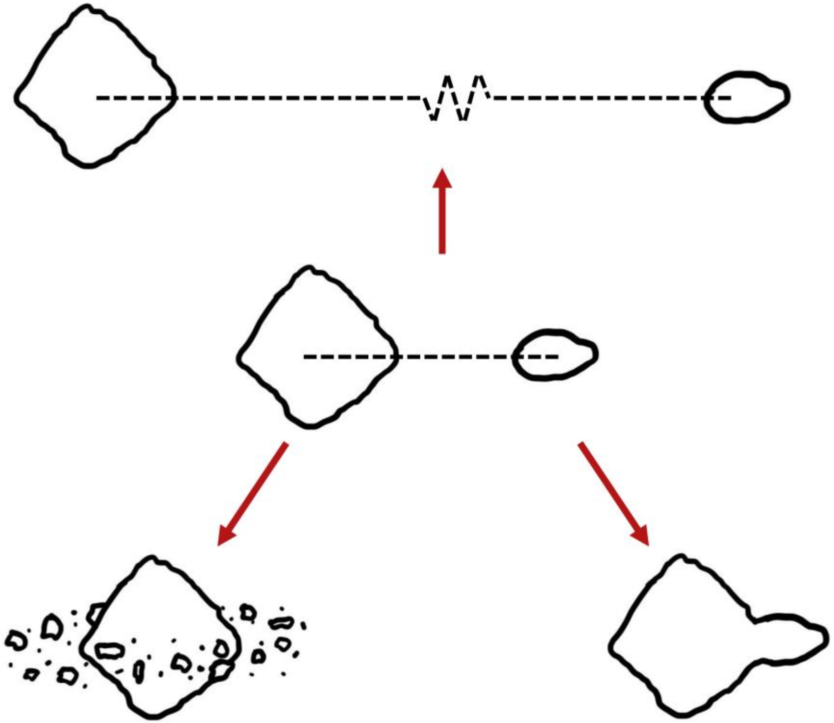

Contact Binaries (CB)

- More than 10% of all small bodies [12, 13, 14]
  - 30% of NEOs [15]
- Extensive process models, no observations
- Via spacecraft impact, one can **create** a CB
- Binary system
  - Contact speed < V_{esc} [16]

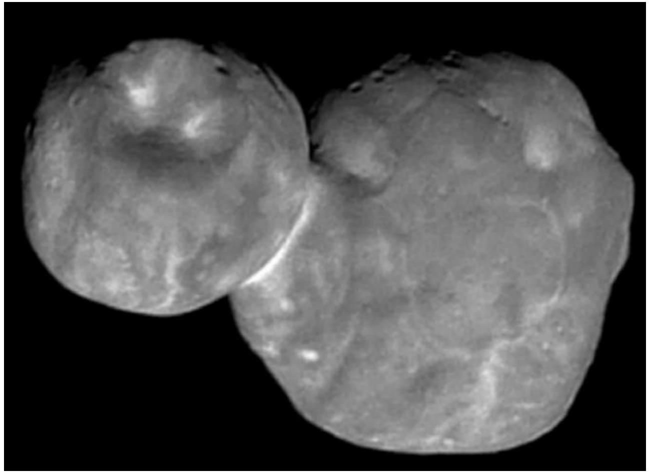

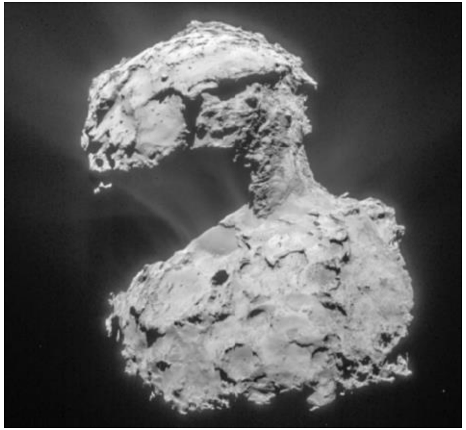

[12] Benner et al., 2006, *Icarus*; [13] Sheppard and Jewitt, 2004, *The Astronomical Journal*; [14] Mann et al., 2007, *The Astronomical Journal*; [15] Virkki et al., *PSJ*, 2022; [16] Jutzi and Asphaug, *Science*, 2015; Images courtesy of NASA, JAXA, ESA

Case Study: (350761) 2002 AW

- Required impact speed of < 2.69 km/s [17]
  - Dimorphos = 488 km/s
- Leaner DART (Impactor) & Hera (Observer) [3, 18]
  - Impactor wet = 1465 kg
  - Observer wet = 995 kg
  - Falcon 9 margin = 200 kg

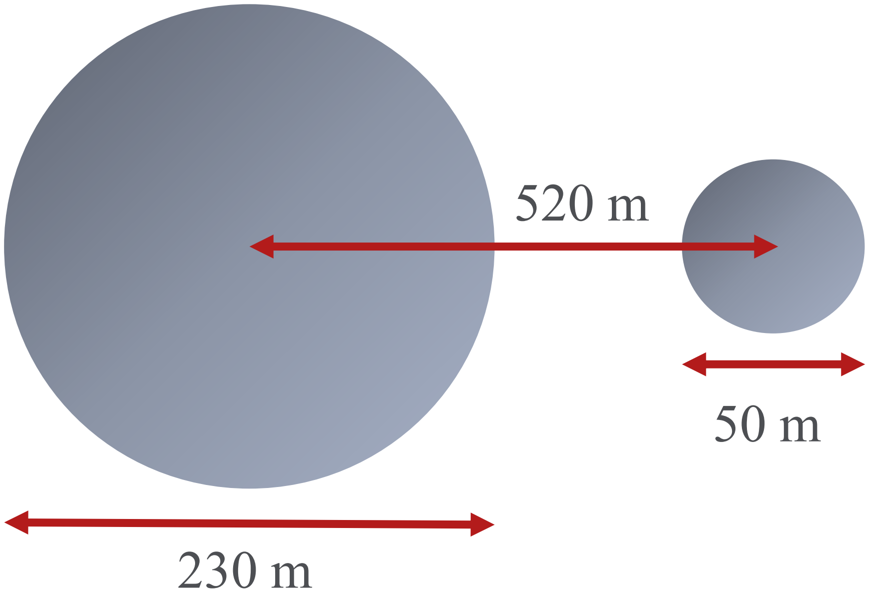

[17] Johnston, W. R., Johnston's Archive, 2022 ; [3] Chabot et al., 2024, *PSJ*; [18] Michel et al., 2022, *PSJ*

Contact Binary Mission Anatomy

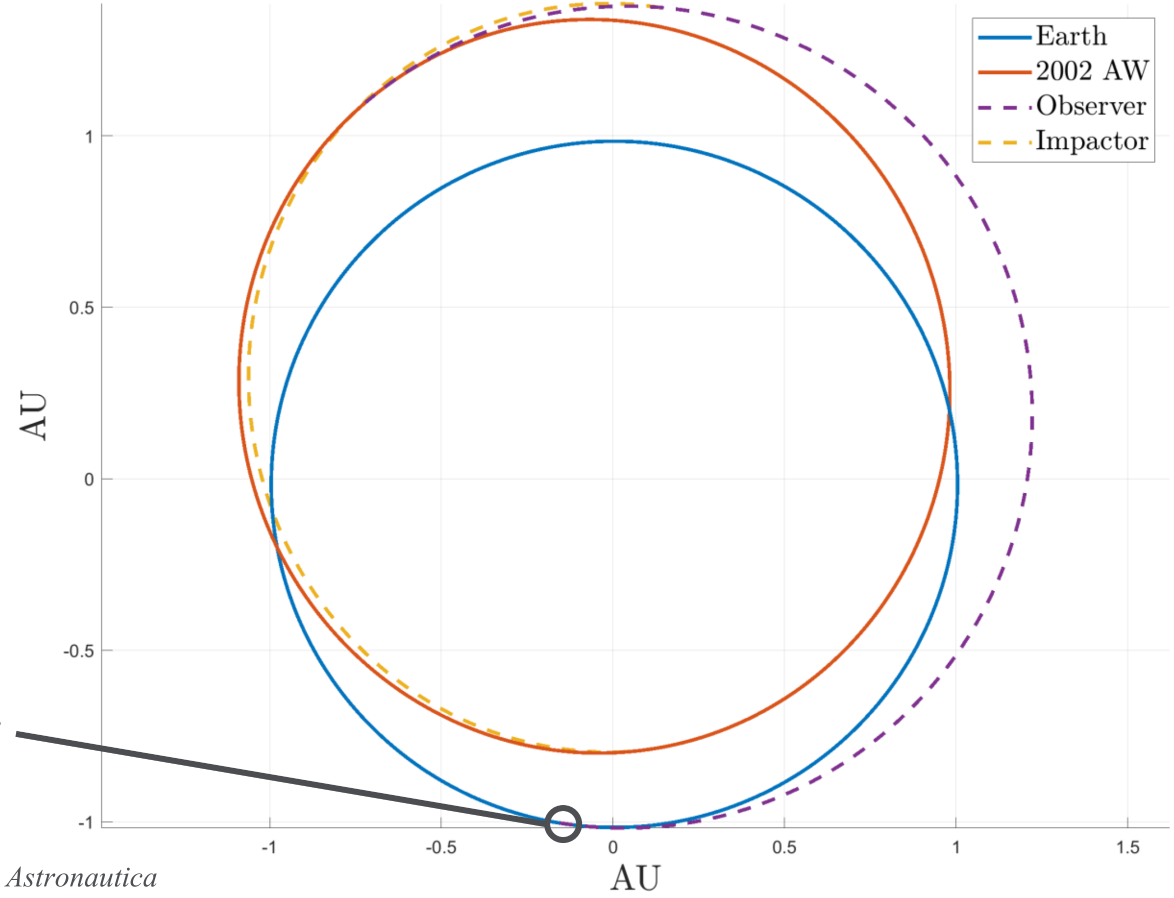

(1) Impactor and Observer launch

[19] Merrill et al., 2024, *Acta Astronautica*

Contact Binary Mission Anatomy

(2) Impactor maneuver

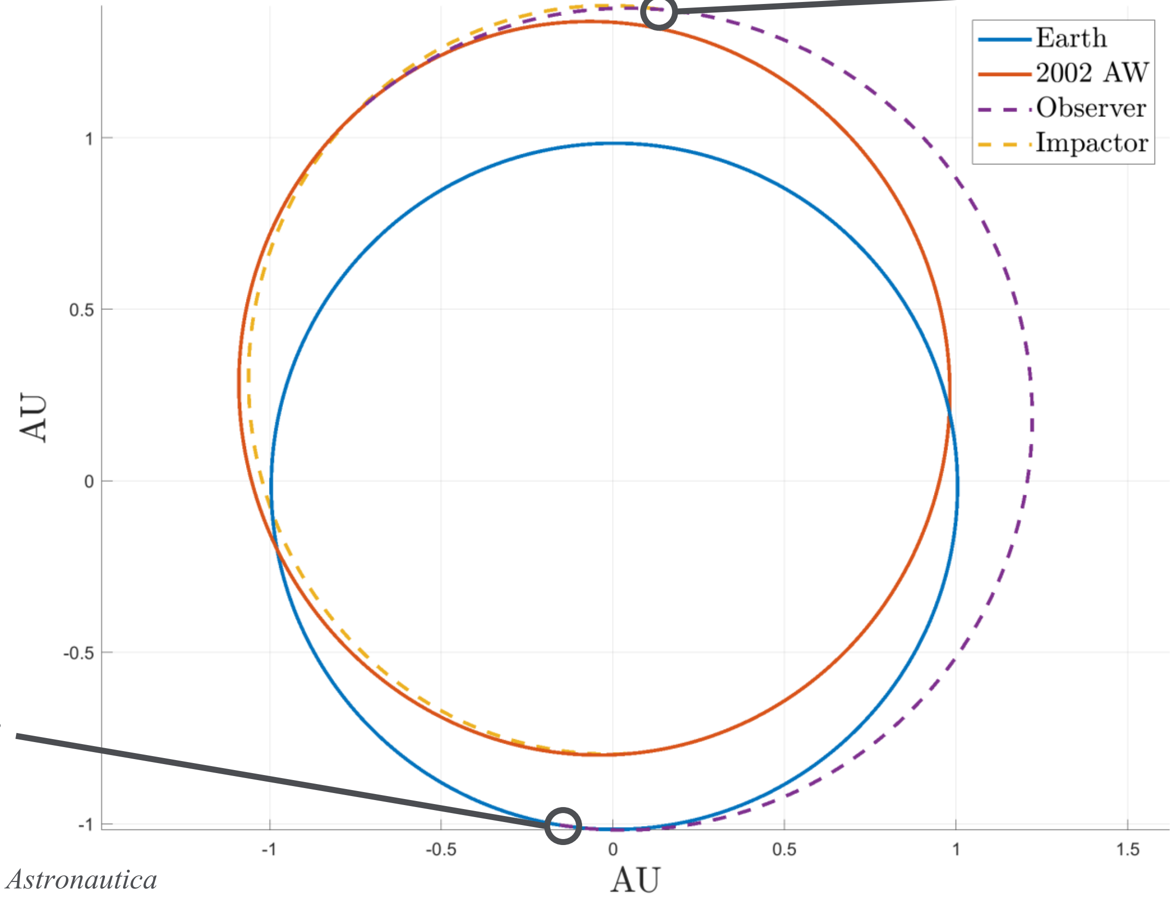

(1) Impactor and Observer launch

[19] Merrill et al., 2024, *Acta Astronautica*

Contact Binary Mission Anatomy

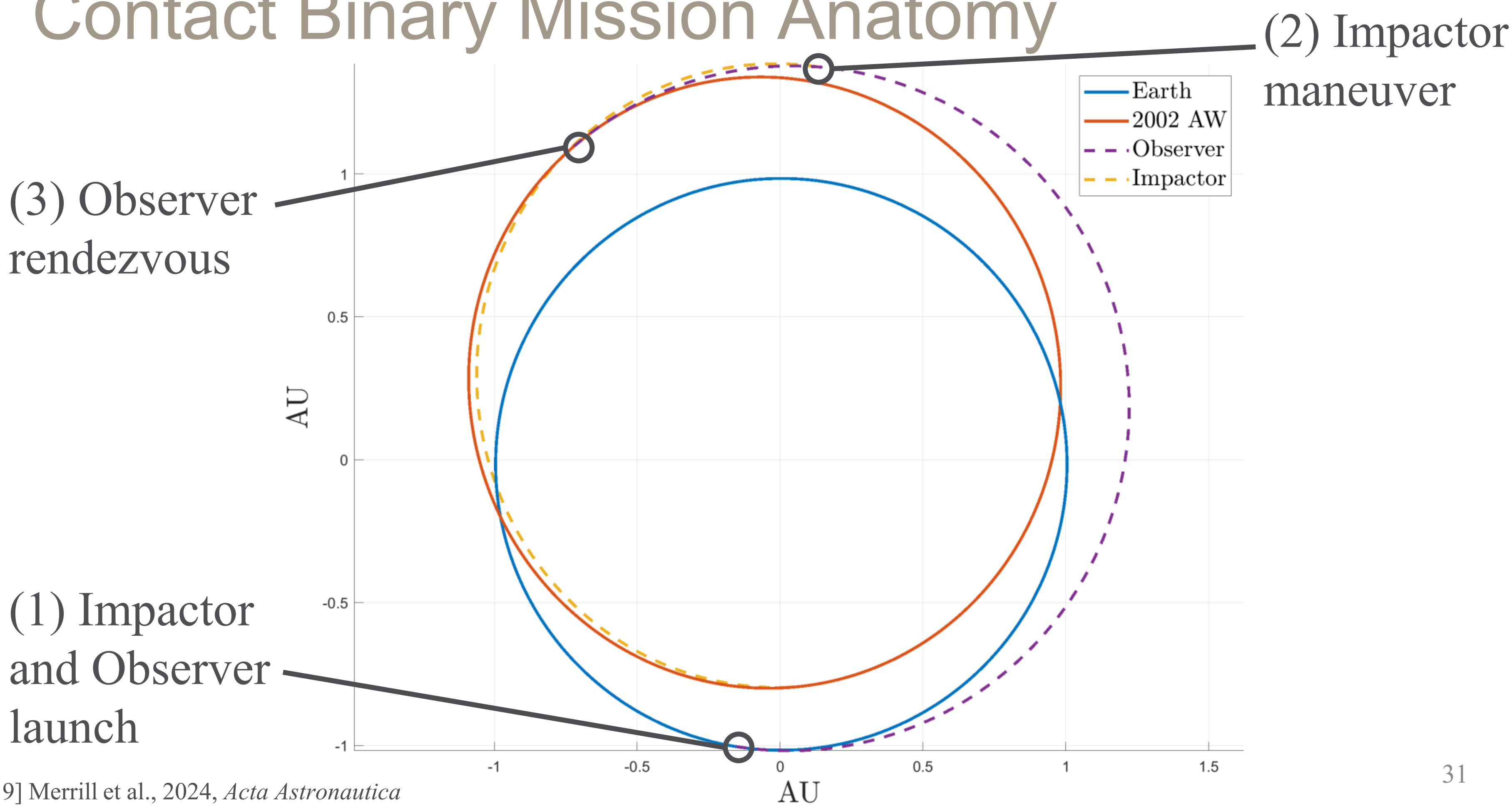

[19] Merrill et al., 2024, *Acta Astronautica*

Contact Binary Mission Anatomy

(3) Observer rendezvous

(1) Impactor and Observer launch

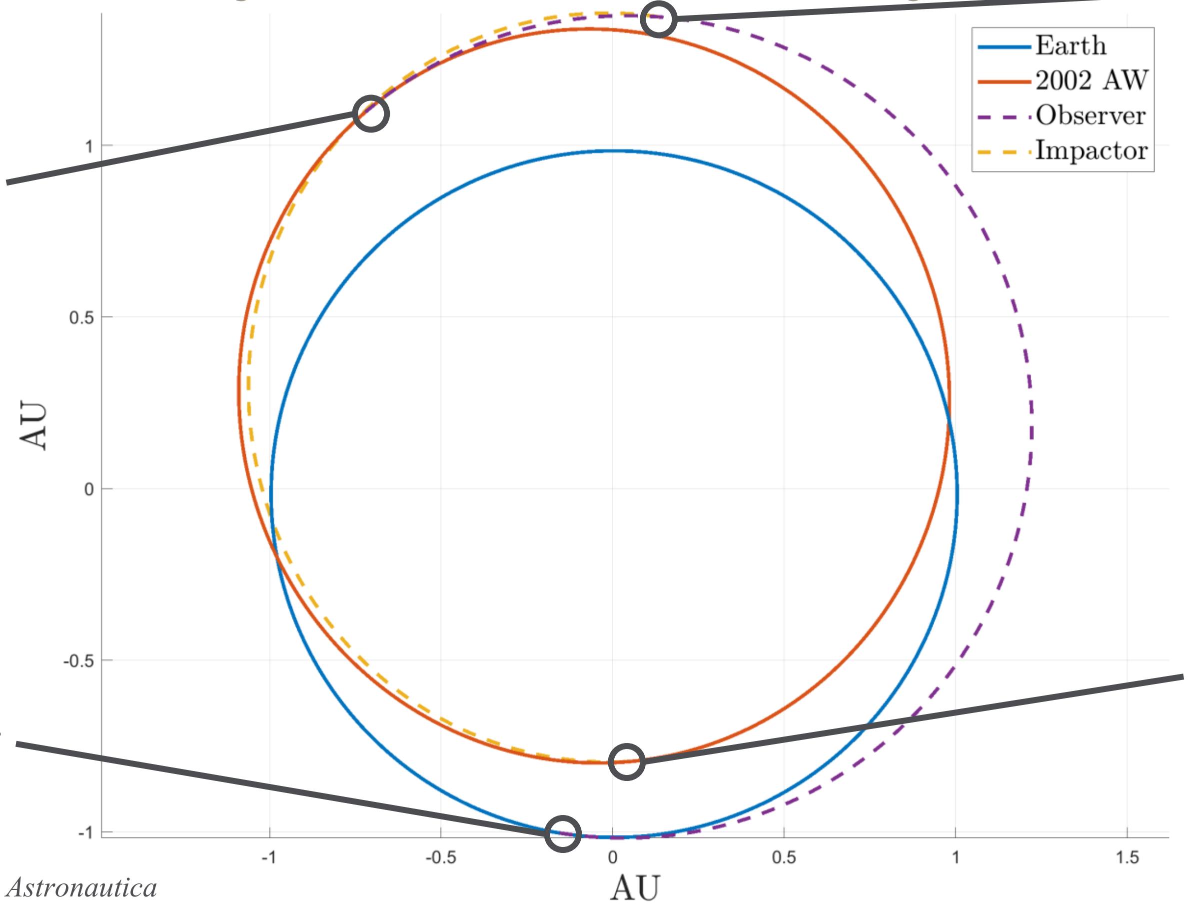

(2) Impactor maneuver

(4) Impact to secondary

[19] Merrill et al., 2024, *Acta Astronautica*

Transfer Orbit Design

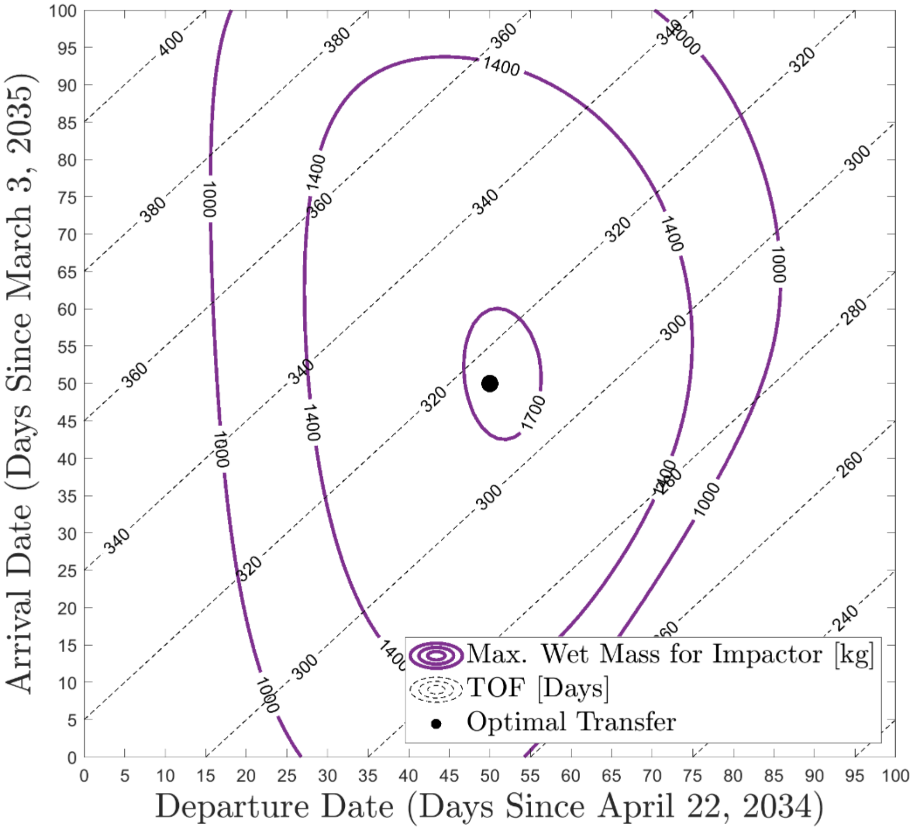

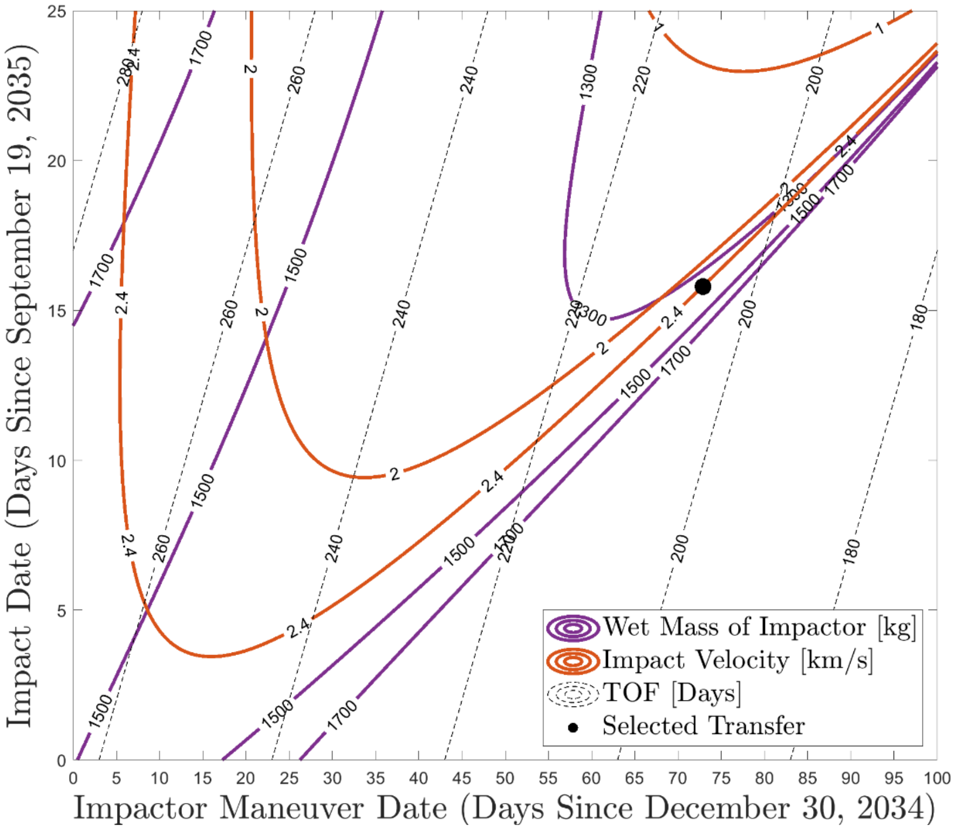

[19] Merrill et al., 2024, *Acta Astronautica*

Momentum Enhancement Factor: β

- The β factor will increase the effect of momentum
- Bounds exist for a min. and max. β value

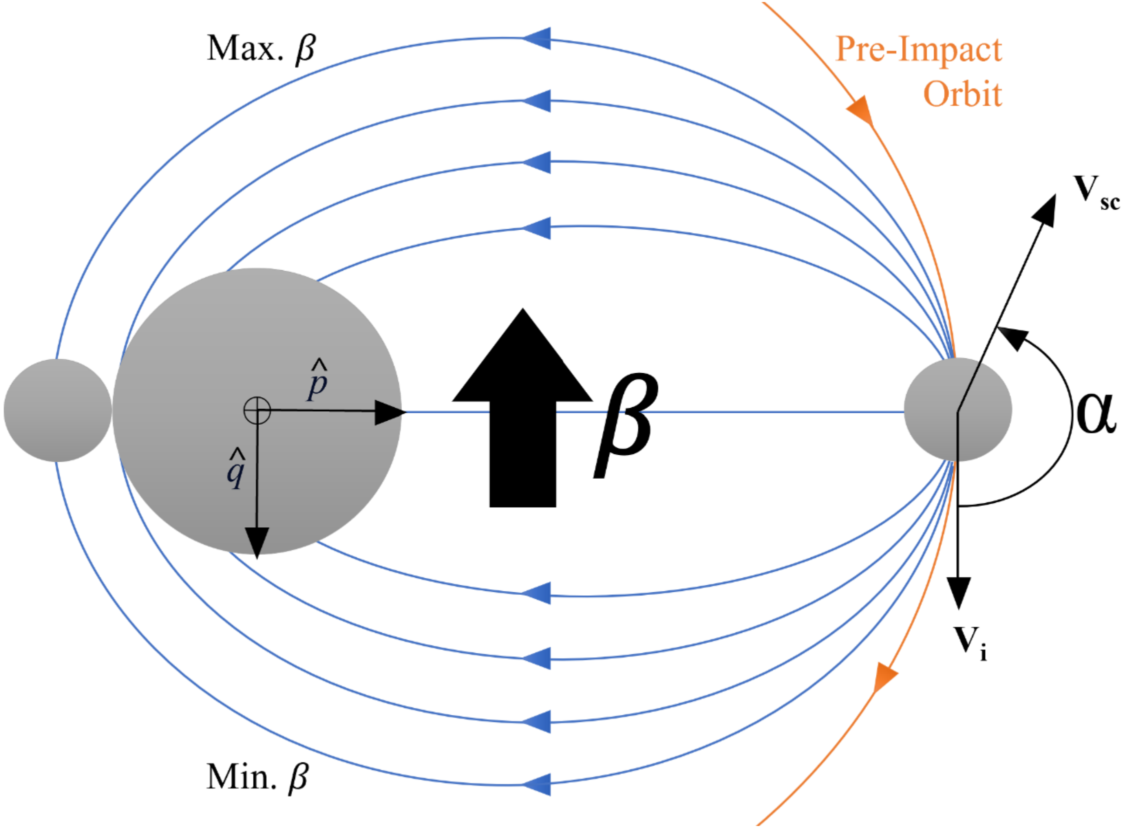

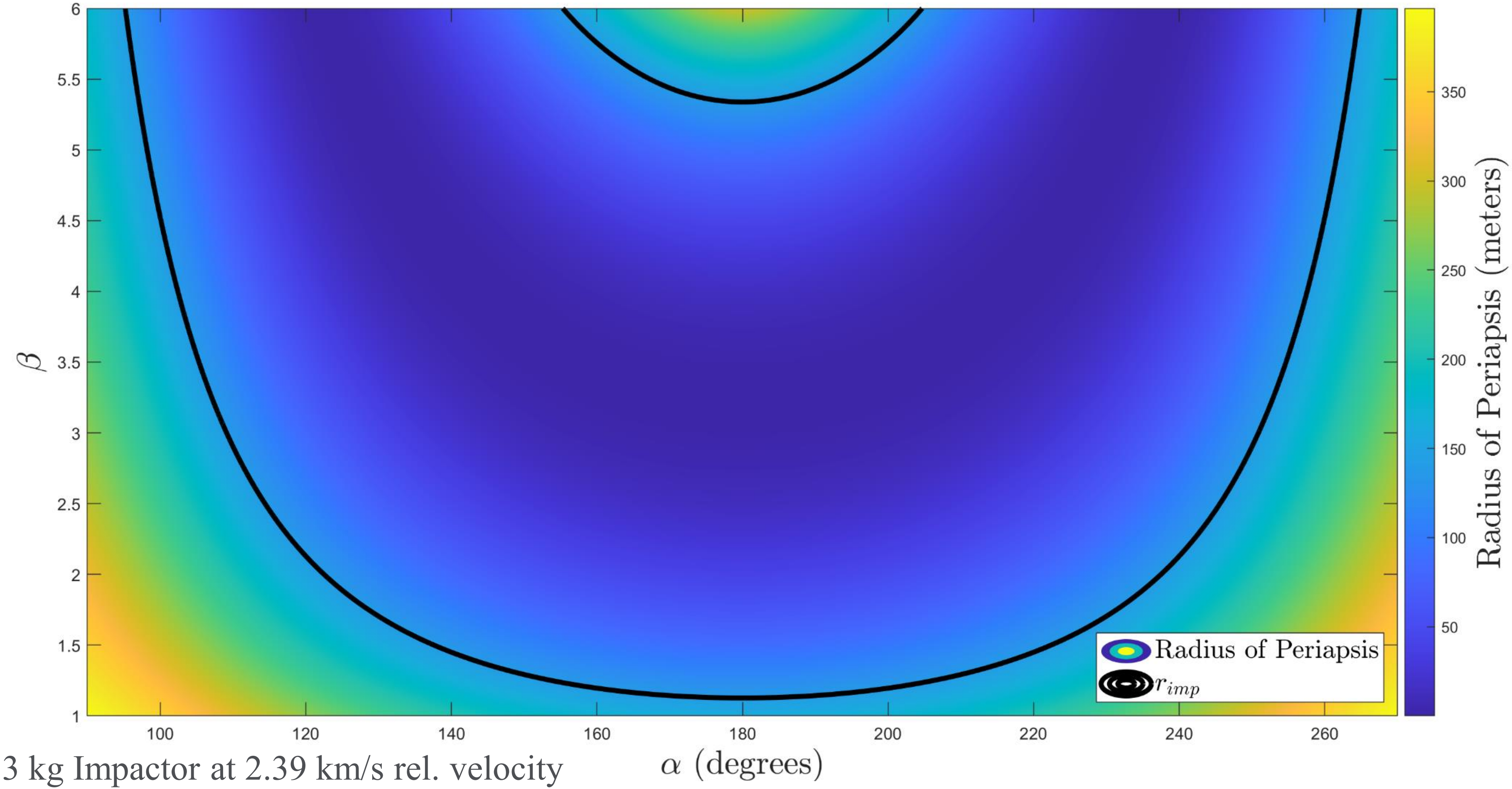

483 kg Impactor at 2.39 km/s rel. velocity

[19] Merrill et al., 2024, *Acta Astronautica*

Gravity Tractor

- Slower effects available from a hovering gravity tractor
- Initial investigation via Gauss equations

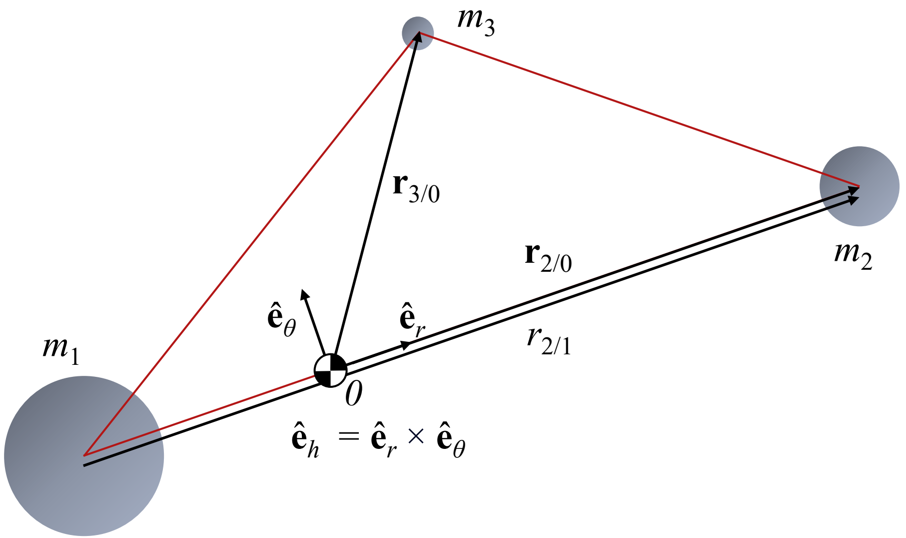

$$\ddot{\mathbf{r}}_{2/0} = -\frac{G(m_1 + m_2)}{r_{2/1}^3}\mathbf{r}_{2/1} + f_r\hat{\mathbf{e}}_r + f_\theta\hat{\mathbf{e}}_\theta + f_h\hat{\mathbf{e}}_h$$

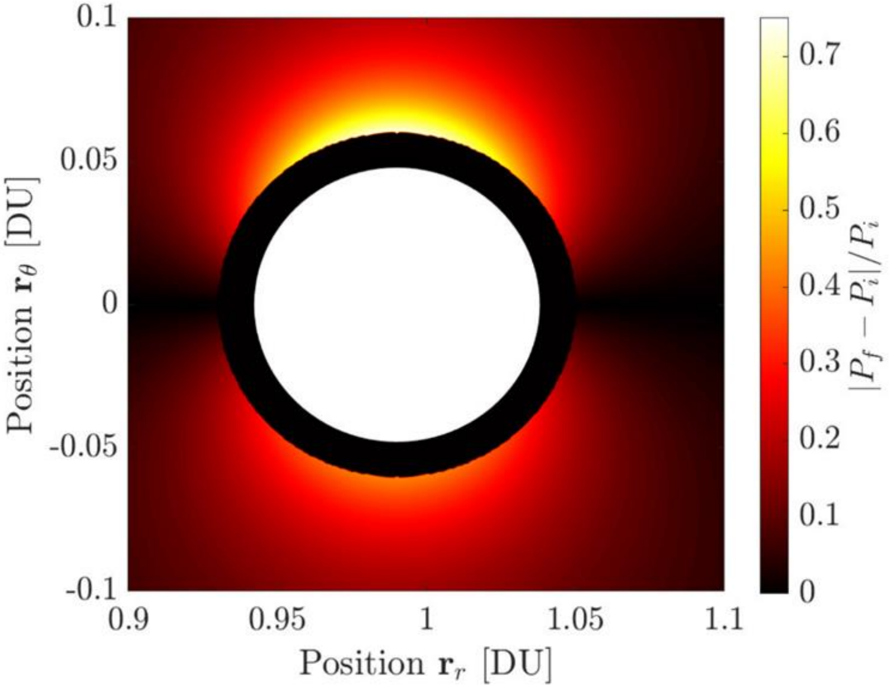

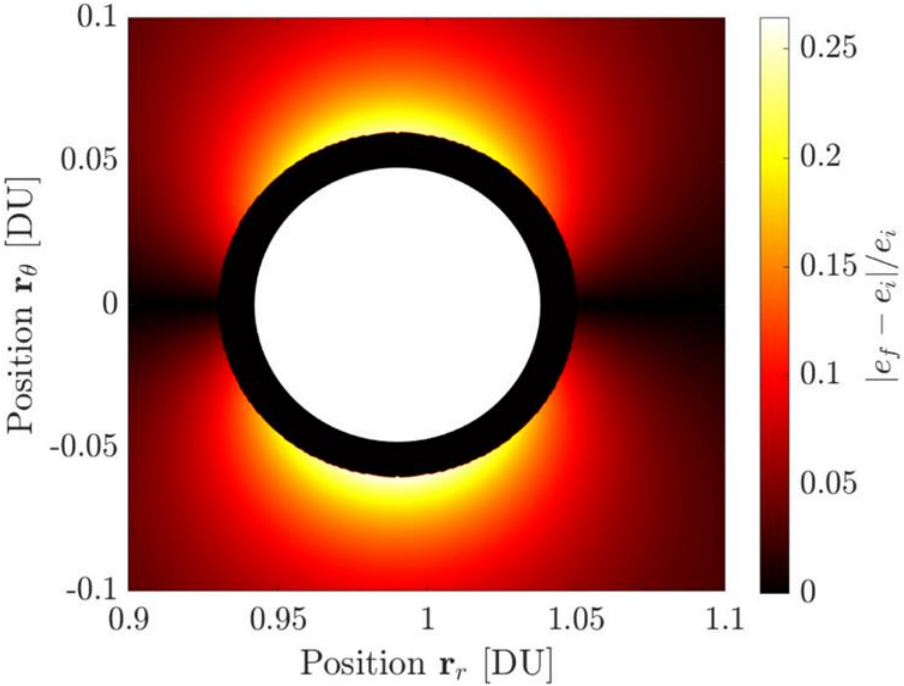

$$\dot{a} = \sqrt{\frac{4a^3}{\mu(1-e^2)}}\left[e\sin(\nu)f_r + (e\cos(\nu)+1)\,f_\theta\right]$$

$$\dot{e} = \sqrt{\frac{a(1-e^2)}{\mu}}\left[\sin(\nu)f_r + \left(\cos(\nu) + \frac{e+\cos(\nu)}{1+e\cos(\nu)}\right)f_\theta\right]$$

Topic 3 Findings

- Spacecraft effects can reproduce binary asteroid evolutionary processes
- A mission to create a contact binary via impact is **currently feasible**
- A gravity tractor demonstration mission is **nearly feasible** but is not optimized

Conclusions

- [Natural] Created new aging method for binary asteroids
- [Artificial] Generated new energy-optimal periodic trajectories in CR3BP
- [Nat+Art] Demonstrated that binary evolution can be reproduced with a spacecraft

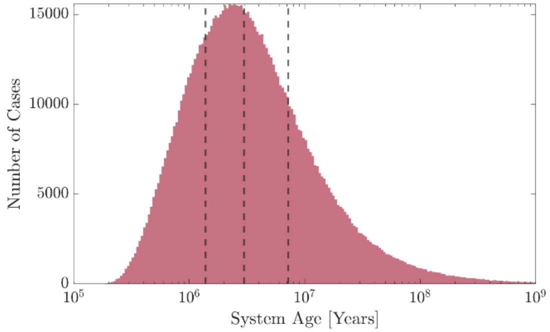

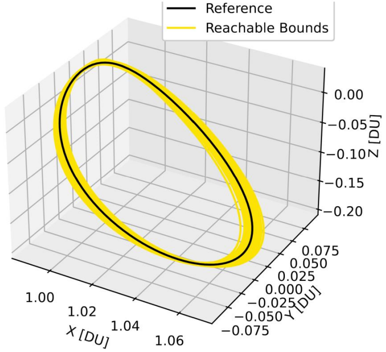

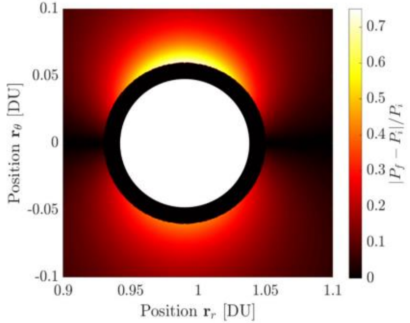

Future Work

- [Natural] Apply aging method to all binary asteroids in equilibrium
- [Artificial] Turn "energy-optimal" trajectories in CR3BP into "fuel-optimal" in a high-fidelity model
- [Nat+Art] Design (optimal) orbits for a gravity tractor in a binary system

Courses

<u>Teaching Assistantships:</u>
ASTRO 1102 – Our Solar System
MAE 3260 – System Dynamics

<u>Technical Courses:</u>
ASTRO 6570 – Physics of the Planets
ASTRO 6577 – Planetary Surface Processes (Audit)
ECE 5210 – Theory of Linear Systems
MAE 5065 – Introduction to Spaceflight Mechanics
MAE 5780 – Feedback Control Systems
MAE 5730 – Intermediate Dynamics
MAE 6720 – Advanced Astrodynamics (Coming Semester)
MAE 6760 – Model-Based Estimation

<u>Other:</u>
LGBT 3635 – Queer Classics (Audit; Coming Semester)
MAE 6949 – MAE Seminar
MAE 7999 – MAE Colloquium (x2)
VIEN 1102 – Introduction to Wines & Vines

Presentations

Invited Talks:
- *The Aerospace Corporation UPLIFT Seminar*, Jun. 2024
- *NASA Lucy Mission Science Team Meeting Presentation*, May 2024
- *University of Maryland Department of Astronomy Center for Theory and Computing Seminar*, Feb. 2024
- *Johns Hopkins University Applied Physics Laboratory Seminar*, Nov. 2022

Conference Presentations:
- **Merrill, C. C.**, Kulik, J., Savransky, D., "Investigation of Low-Thrust Enabled State Return Trajectories in the CR3BP," *2024 AAS/AIAA Astrodynamics Specialist Conference,* 2024. Oral Presentation.
- **Merrill, C. C.**, Savransky, D., "Investigating Orbits for a Gravity Tractor Demonstration Mission," *13th Annual oSTEM Conference,* 2023. Poster Presentation.
- **Merrill, C. C.** "Creating a Contact Binary via Spacecraft Impact: The Effects of Eccentricity," *29th Meeting of the Small Bodies Assessment Group*, 2023. Oral Presentation.
- **Merrill, C. C.**, Geiger, C. J., Tahsin, A. T. M., Banginwar, P., Peck, M., and Savransky, D. "Mission Design to Create a Contact Binary via Spacecraft Impact to Near-Earth Binary Asteroid (350751) 2002 AW," *8th International Planetary Defense Conference*, 2023. Oral Presentation.

Publications

Conference:

- **Merrill, C. C.**, Kulik, J., and Savransky, D. "Generation of Energy-Optimal Low-Thrust Forced Periodic Structures in the CR3BP," *2024 AAS/AIAA Astrodynamics Specialist Conference,* 2024.

Journal:

- **Merrill, C. C.**, Kubas, A. R., Meyer, A. J., and Raducan, S. D. "Age of (152830) Dinkinesh I Selam constrained by secular tidal-BYORP theory," *Astronomy and Astrophysics*, 2024. 10.1051/0004-6361/202449716
- **Merrill, C. C.**, Geiger, C. J., Tahsin, A. T. M., Savransky, D., and Peck, M. "Creating a Contact Binary via Spacecraft Impact to Near-Earth Binary Asteroid (350751) 2002 AW," *Acta Astronautica*, 2024. 10.1016/j.actaastro.2023.11.030

Contributing Author:

- Ferrari, F., and 32 colleagues incl. **Merrill, C. C.** "Morphology of ejecta features from the DART impact on Dimorphos and their implications," *Nature Communications*, Submitted.
- Hirabayashi, M., and 75 colleagues incl. **Merrill, C. C.** "Kinetic deflection change due to target global curvature as revealed by NASA/DART," *Nature Communications*, Submitted.
- Richardson, D. C., and 52 colleagues incl. **Merrill, C. C.** "The Dynamical State of the Didymos System Before and After the DART Impact," *The Planetary Science Journal*, 2024. 10.3847/PSJ/ad62f5
- Nakano, R., and 19 colleagues incl. **Merrill, C. C.** "Dimorphos's Orbit Period Change and Attitude Perturbation due to Its Reshaping after the DART Impact," *The Planetary Science Journal*, 2024. 10.3847/PSJ/ad4350
- Raducan, S., and 6 colleagues incl. **Merrill, C. C.** "Lessons learned from NASA's DART impact about disrupting rubble-pile asteroids," *The Planetary Science Journal*, 2024. 10.3847/PSJ/ad29f6
- Chabot, N. L., and 128 colleagues incl. **Merrill, C. C.** "Achievement of the Planetary Defense Investigations of the Double Asteroid Redirection Test (DART) Mission," *The Planetary Science Journal*, 2024. 10.3847/PSJ/ad16e6
- Cueva, R. H., and 7 colleagues incl. **Merrill, C. C.** "The Secular Dynamical Evolution of Binary Asteroid System (65803) Didymos Post-DART," *The Planetary Science Journal*, 2024. 10.3847/PSJ/ad2173
- Meyer, A. J., and 22 colleagues incl. **Merrill, C. C.** "The Perturbed Full Two-Body Problem: Applications to Post-DART Didymos," *The Planetary Science Journal*, 2023. 10.3847/PSJ/acebc7

Acknowledgements

Thank you to my family, friends, colleagues, mentors, and committee members for all your support!

See you at the B! (hopefully before then, too)

References

[1] Pravec et al., 2006, *Icarus*, doi.org/10.1016/j.icarus.2005.10.014
[2] Walsh et al., 2008, *Nature*, doi.org/10.1038/nature07078
[3] Chabot et al., 2024, *PSJ*, doi.org/10.3847/PSJ/ad16e6
[4] Levison et al., 2024, *Nature*, doi.org/10.1038/s41586-024-07378-0
[5] Agrusa et al., 2024, *PSJ*, doi.org/10.3847/PSJ/ad206b
[6] McMahon and Scheeres, 2010, *Icarus*, doi.org/10.1016/j.icarus.2010.05.016
[7] Murray and Dermott, 1999
[8] Rossi et al., 2009, *Icarus*, doi.org/10.1016/j.icarus.2009.02.030
[9] Merrill et al., 2024, *A&A*
[10] Marchi, *personal communication*
[11] Savransky, *personal communication*
[12] Benner et al., 2006, *Icarus*, doi.org/10.1016/j.icarus.2006.01.016
[13] Sheppard and Jewitt, 2004, *The Astronomical Journal*, doi.org/10.1086/383558
[14] Mann et al., 2007, *The Astronomical Journal*, doi.org/10.1086/520328
[15] Virkki et al., 2022, *PSJ*, doi.org/10.3847/PSJ/ac8b72
[16] Jutzi and Asphaug, 2015, *Science*, doi.org/10.1126/science.aaa4747
[17] Johnston, 2022, *Johnston's Archive*
[18] Michel et al., 2022, *PSJ*, doi.org/10.3847/PSJ/ac6f52
[19] Merrill et al., 2024, *Acta Astronautica*

Images courtesy of NASA, JAXA, and ESA

Parameter	Didymos [a]	Dinkinesh [b]
Volume-equivalent diameter of primary [m]	730 ± 17	719 ± 24
Volume-equivalent diameter of secondary [m]	150.0 ± 2.5	282 ± 28
Bulk density of primary, secondary [kg m^{-3}]	2790 ± 140, 2400 ± 300	2400 ± 350
Semi-major axis [m]	1189 ± 17	3110 ± 50
Secondary shape	Oblate ellipsoid	Bilobate
Mutual orbital period [h]	11.921493 ± 0.000016	52.67 ± 0.04
Mutual orbital eccentricity	<0.03	0
Primary rotation period [h]	2.2600 ± 0.0001	3.7387 ± 0.0013
Heliocentric semi-major axis [AU]	1.64266506 [c]	2.1915426 [c]
Heliocentric eccentricity	0.383264789 [c]	0.1121065 [c]

Secular Equations of Motion

BYORP and tides affect **Selam's orbit**[6, 7]

$$\dot{a}_{\mathrm{B}} = \frac{3H_{\odot}}{2\pi\rho_{\mathrm{s}}R_{\mathrm{s}}}\sqrt{\frac{a^3(1-e^2)}{\mu}}\,B \qquad \dot{a}_{\mathrm{T}} = sign(\omega_{\mathrm{p}} - n)3n\frac{k}{Q}\frac{M_{\mathrm{s}}}{M_{\mathrm{p}}}\frac{R_{\mathrm{p}}^5}{a^4}$$

YORP and tides affect **Dinkinesh's spin**[7, 8]

$$\dot{\omega}_{\mathrm{p,Y}} = \frac{H_{\odot}}{2\pi R_{\mathrm{p}}^2\rho_{\mathrm{p}}}C_{\mathrm{Y}} \qquad \dot{\omega}_{\mathrm{p,T}} = -sign(\omega_{\mathrm{p}} - n)\frac{3k}{2\alpha Q}\frac{GM_{\mathrm{s}}^2R_{\mathrm{p}}^3}{M_{\mathrm{p}}a^6}$$

[6] McMahon and Scheeres, 2010, *Icarus*; [7] Murray and Dermott, 1999; [8] Rossi et al., 2009, *Icarus*

Equilibria

$$C_{\mathrm{Y}} = -B \frac{2\pi\rho_{\mathrm{p}}^3 a_{\mathrm{eq}} G R_{\mathrm{s}}^2}{\rho_{\mathrm{s}}^2 \mu \alpha}$$

$$a_{\mathrm{eq}} = \left(\frac{k}{|B|Q} \frac{2\pi\rho_{\mathrm{s}}^2 \mu R_{\mathrm{p}}^2 R_{\mathrm{s}}^4}{\rho_{\mathrm{p}} H_{\odot}} \right)^{1/7}$$

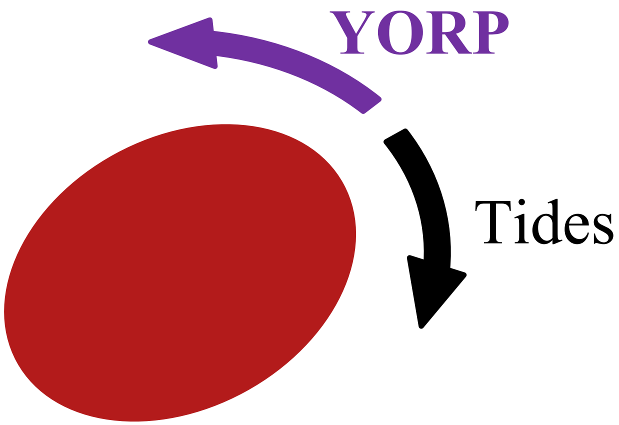

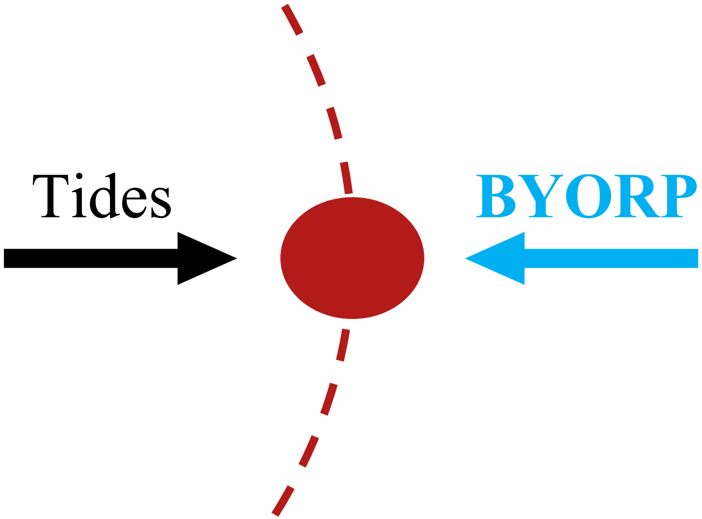

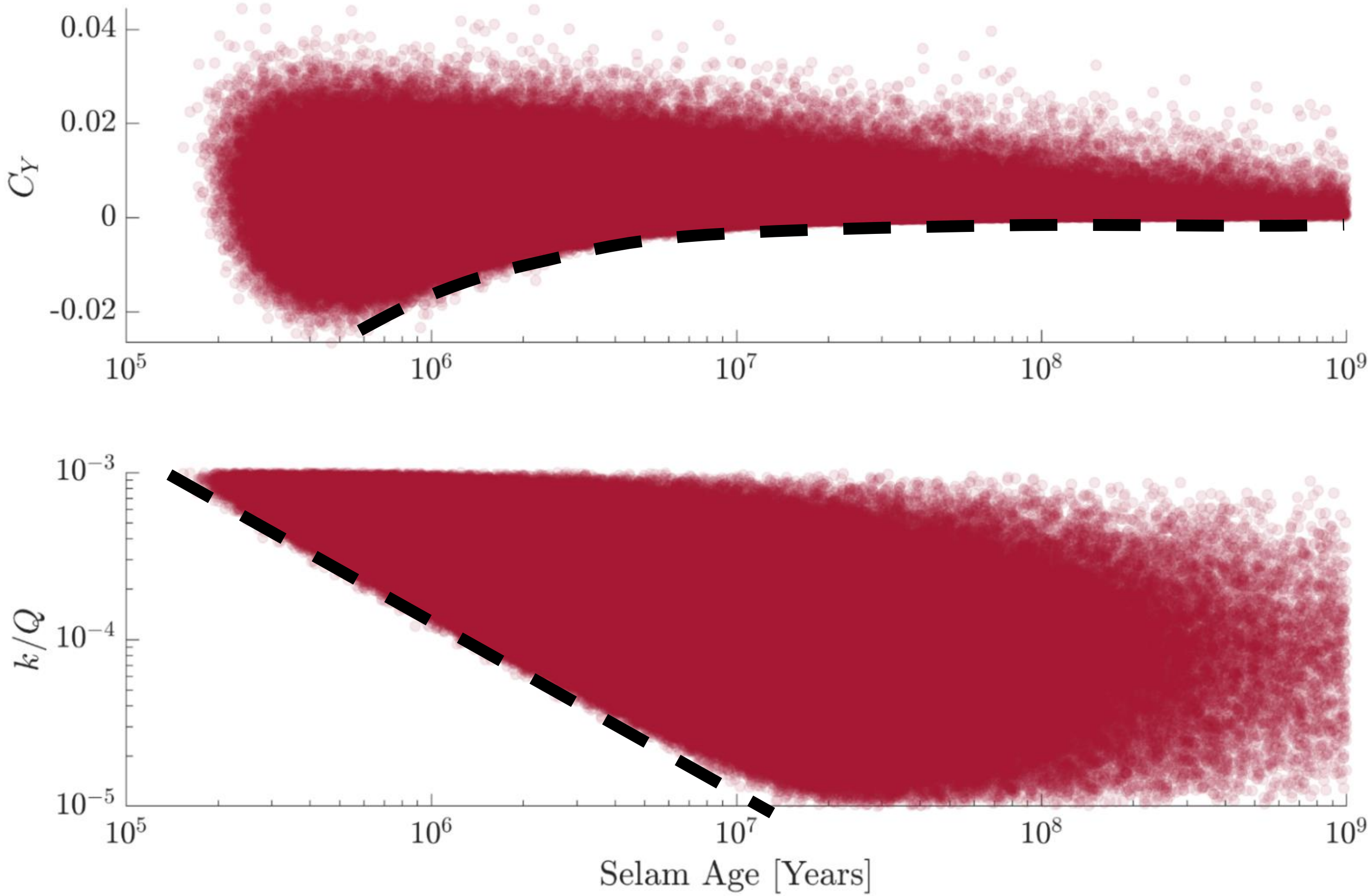

$\dot{\omega} \propto C_Y$

$\dot{a} \propto k/Q$

k/Q = 1e-4 C_Y = 1.7e-3 Age = 2.007 Ma

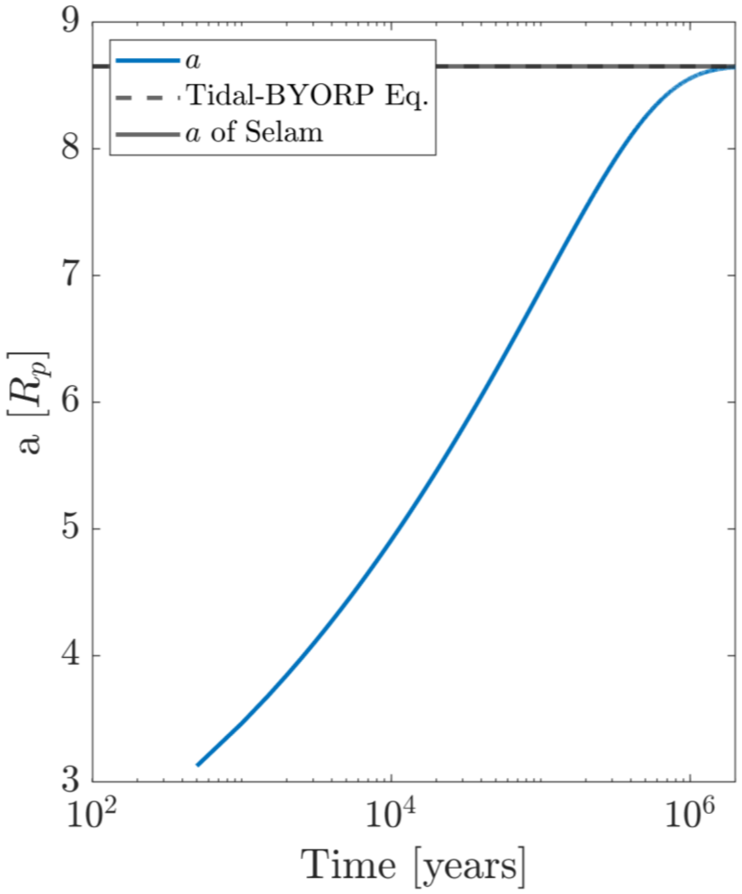

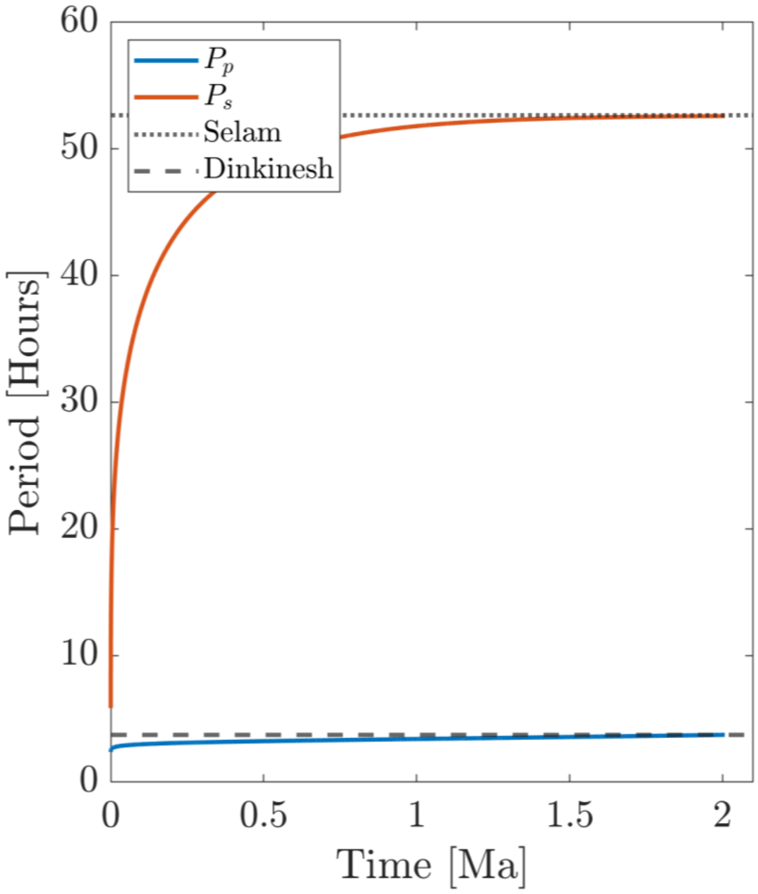

Parameter	Variable type	Mean value $\pm 1\sigma$; [bounds]	Note and source
Final mutual orbit period [h]	Fixed	52.67	Mottola et al. (2023)
Eccentricity	Fixed	0	Levison et al. (2024)
Diameter of Dinkinesh [m]	Gaussian	719 ± 24	Levison et al. (2024)
Diameter of Selam [m]	Gaussian	282 ± 28	Levison et al. (2024)
a_{eq} [m]	Gaussian	3110 ± 50	Levison et al. (2024)
k/Q	Log-Uniform	10^{-x}; $x \in (3, 5)$	x is uniformly distributed
Coefficient for YORP	Gaussian	0 ± 0.0125 ; [−2, Eq. (14)]	Rossi et al. (2009)
Coefficient for BYORP	Derived	Eq. (11)	Contractive BYORP only
Density [$\mathrm{kg\,m^{-3}}$]	Derived	$3\pi a_{eq}^3/(P^2 G(R_p^3 + R_s^3))$	–
Initial primary spin [$\mathrm{rad\,s^{-1}}$]	Derived	Eq. (15)	Angular momentum conservation
Initial semi-major axis [m]	Uniform	$(1.5R_p\,,\,2.5R_p)$	Roche limit

Some Extra Notes

- 88% of angular momentum content indicates that BYORP+YORP have decreased the net ang. mom.
  - Supports YORP spin-down
  - Supports contractive BYORP
- Model outputs:
  - $\mu = 33.1 \pm 1.6$ m^3 s^{-2}
  - $\rho = 2420 \pm 1.6$ kg m^{-3}

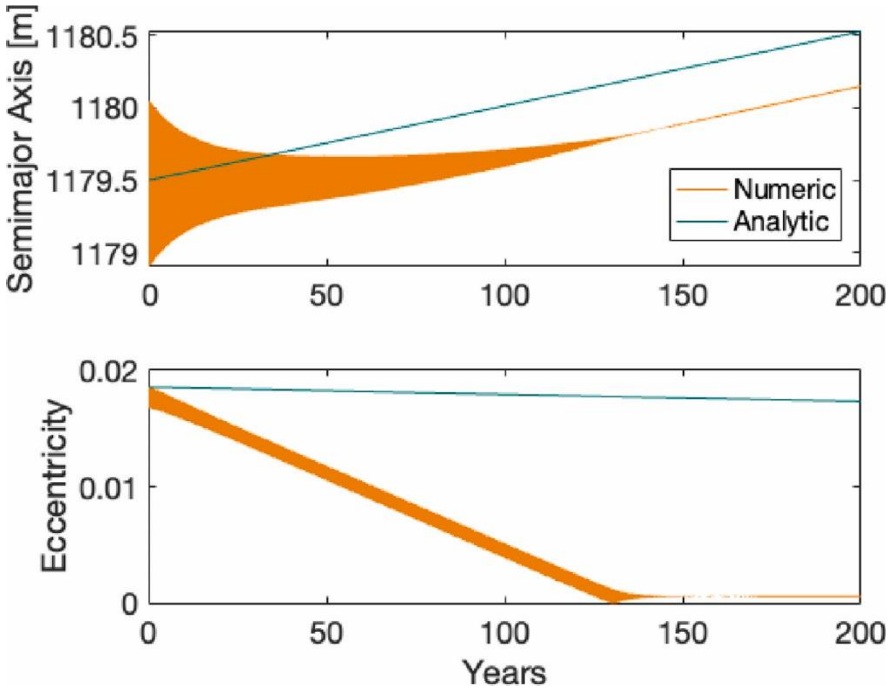

$$\dot{\theta}^* = \sqrt{\frac{\mu}{r^3}\left(1 + \frac{3(\bar{I}_{A,z} - \bar{I}_{A,xy} - 2\bar{I}_{B,x} + \bar{I}_{B,y} + \bar{I}_{B,z})}{2r^2}\right)}$$

$$\omega_\mathrm{p} = \frac{\alpha(M_\mathrm{p} + M_\mathrm{s})(R_\mathrm{p}^3 + R_\mathrm{s}^3)^{2/3}\omega_\mathrm{d} - M^* \sqrt{\mu a_\mathrm{i}} - \alpha M_\mathrm{s} R_\mathrm{s}^2 n}{\alpha M_\mathrm{p} R_\mathrm{p}^2}$$

$$a_\mathrm{eq} = \left(\frac{k}{|B|Q} \frac{2\pi\rho_\mathrm{s}^2 \mu R_\mathrm{p}^2 R_\mathrm{s}^4}{\rho_\mathrm{p} H_\odot} \right)^{1/7}$$

$$a_\mathrm{Y} = \left| \frac{k}{C_\mathrm{Y} Q} \frac{4\pi^2 G R_\mathrm{p}^2 R_\mathrm{s}^6 \rho_\mathrm{p}^2}{H_\odot \alpha} \right|^{1/6}$$

$$\frac{|B|Q}{k} = \frac{2\pi\rho_\mathrm{s}^2 \mu R_\mathrm{p}^2 R_\mathrm{s}^4}{\rho_\mathrm{p} H_\odot a_\mathrm{eq}^7}$$

$$C_\mathrm{Y} = -B \frac{2\pi\rho_\mathrm{p}^3 a_\mathrm{eq} G R_\mathrm{s}^2}{\rho_\mathrm{s}^2 \mu \alpha}$$

$$\mathbf{F}(\mathbf{x}) = \begin{bmatrix} v_x \\ v_y \\ v_z \\ 2v_y + x - (1-\mu^*)\frac{x+\mu^*}{R_1^3} - \mu^*\frac{x-1+\mu^*}{R_2^3} \\ -2v_x + y - (1-\mu^*)\frac{y}{R_1^3} - \mu^*\frac{y}{R_2^3} \\ -(1-\mu^*)\frac{z}{R_1^3} - \mu^*\frac{z}{R_2^3} \end{bmatrix}$$

$$R_2 = \sqrt{(x-1+\mu^*)^2 + y^2 + z^2}$$

$$R_1 = \sqrt{(x+\mu^*)^2 + y^2 + z^2}$$

$$\mathbf{a}_i = \sqrt{\frac{J^*}{\gamma_i}}\mathbf{w}_i$$

$$J = \frac{1}{2}\int_{t_0}^{t_f} ||\mathbf{u}||^2 dt$$

$$\delta\mathbf{y}(t_f) = \begin{bmatrix} \delta\mathbf{r}(t_f) \\ \delta\mathbf{v}(t_f) \\ \delta\boldsymbol{\lambda}_r(t_f) \\ \delta\boldsymbol{\lambda}_v(t_f) \end{bmatrix} = \boldsymbol{\Phi}(t_f, t_0)\delta\mathbf{y}_0 = \begin{bmatrix} \boldsymbol{\Phi}_{\mathbf{x}}^{\mathbf{x}} & \boldsymbol{\Phi}_{\boldsymbol{\lambda}}^{\mathbf{x}} \\ \boldsymbol{\Phi}_{\mathbf{x}}^{\boldsymbol{\lambda}} & \boldsymbol{\Phi}_{\boldsymbol{\lambda}}^{\boldsymbol{\lambda}} \end{bmatrix}\delta\mathbf{y}_0 = \begin{bmatrix} \boldsymbol{\Phi}_{\mathbf{r}}^{\mathbf{r}} & \boldsymbol{\Phi}_{\mathbf{v}}^{\mathbf{r}} & \boldsymbol{\Phi}_{\boldsymbol{\lambda}_r}^{\mathbf{r}} & \boldsymbol{\Phi}_{\boldsymbol{\lambda}_v}^{\mathbf{r}} \\ \boldsymbol{\Phi}_{\mathbf{r}}^{\mathbf{v}} & \boldsymbol{\Phi}_{\mathbf{v}}^{\mathbf{v}} & \boldsymbol{\Phi}_{\boldsymbol{\lambda}_r}^{\mathbf{v}} & \boldsymbol{\Phi}_{\boldsymbol{\lambda}_v}^{\mathbf{v}} \\ \boldsymbol{\Phi}_{\mathbf{r}}^{\boldsymbol{\lambda}_r} & \boldsymbol{\Phi}_{\mathbf{v}}^{\boldsymbol{\lambda}_r} & \boldsymbol{\Phi}_{\boldsymbol{\lambda}_r}^{\boldsymbol{\lambda}_r} & \boldsymbol{\Phi}_{\boldsymbol{\lambda}_v}^{\boldsymbol{\lambda}_r} \\ \boldsymbol{\Phi}_{\mathbf{r}}^{\boldsymbol{\lambda}_v} & \boldsymbol{\Phi}_{\mathbf{v}}^{\boldsymbol{\lambda}_v} & \boldsymbol{\Phi}_{\boldsymbol{\lambda}_r}^{\boldsymbol{\lambda}_v} & \boldsymbol{\Phi}_{\boldsymbol{\lambda}_v}^{\boldsymbol{\lambda}_v} \end{bmatrix}\delta\mathbf{y}_0$$

$$\boldsymbol{\Phi}_{\mathbf{a}}^{\mathbf{b}}(t, t_0) = \frac{\partial\mathbf{b}(t)}{\partial\mathbf{a}(t_0)}$$

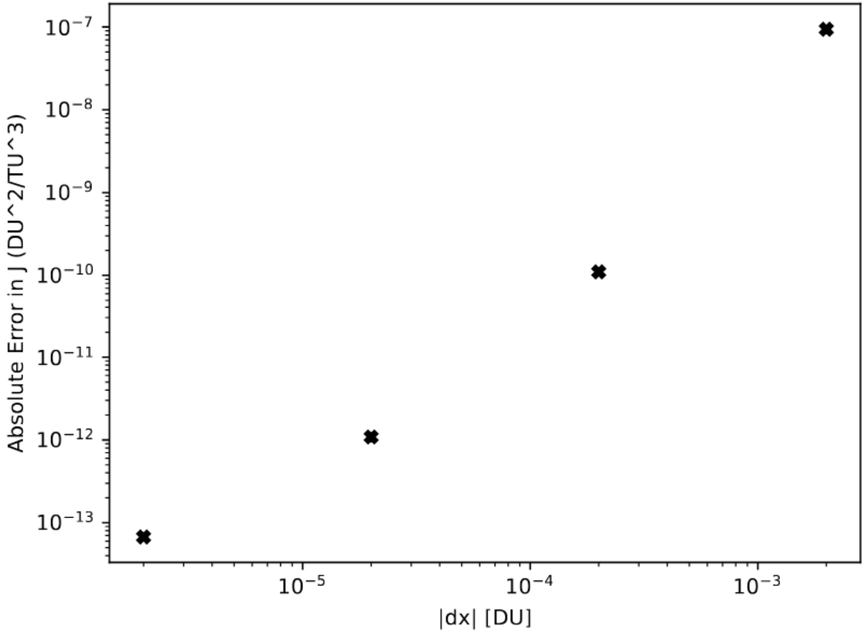
Absolute Error in J (DU^2/TU^3)
10^{-7}
10^{-8}
10^{-9}
10^{-10}
10^{-11}
10^{-12}
10^{-13}
10^{-5}
10^{-4}
10^{-3}
|dx| [DU]

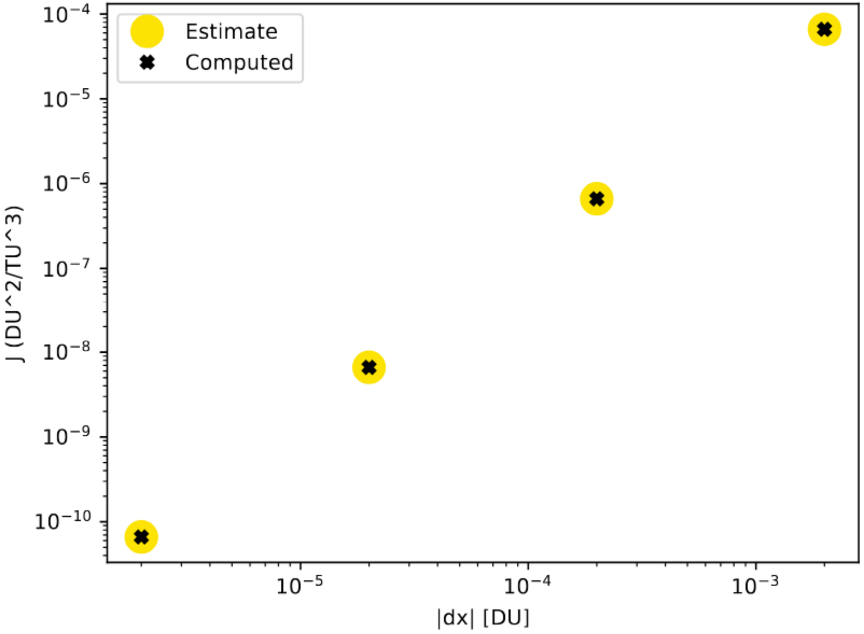
Estimate
Computed
J (DU^2/TU^3)
10^{-4}
10^{-5}
10^{-6}
10^{-7}
10^{-8}
10^{-9}
10^{-10}
10^{-5}
10^{-4}
10^{-3}
|dx| [DU]

(350761) 2002 AW Characteristics

Period of Secondary = 1.05 days [5]

Density = 1580 kg/m^3 (derived)

Mass of Secondary = 10^8 kg (derived)

Mass of Primary = 10^{10} kg (derived)

Heliocentric Data:

P = 405 days	i = 0.575°
e = 0.256	Ω = 162°
ω = 119°	a = 1.07 AU

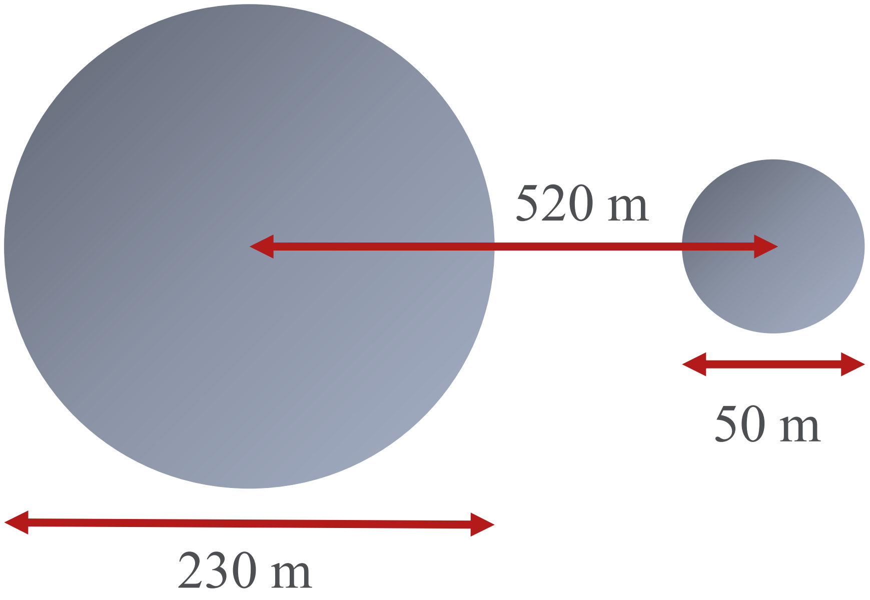

[5] Johnston, W. R., Johnston's Archive, 2022

Table 4
The mass breakdown for this mission design. CBE refers to the current best estimate of the dry mass. The contingency masses are derived from [31,32,40]. Propellant mass is calculated as the mass necessary to perform all maneuvers for the CBE + contingency mass of each component. All propellant calculations use an $I_{sp} = 235$ s.

Impactor	CBE	402 kg
	Contingency	40 kg (10%)
	Propellant	925 kg
	Prop. Contingency	93 kg (10%)
	Total	1460 kg
Observer	CBE	316 kg
	Contingency	104 kg (33%)
	Propellant	523 kg
	Prop. Contingency	52 kg (10%)
	Total	995 kg
Total		**2455 kg**
Falcon 9 launch		**2655 kg**
Mass margin		**200 kg**

Name	Min. V_∞ Required (km/s)	Max. V_∞ Allowed (km/s)	Min. Total ΔV (km/s)	β_{max}/β_{min}
Didymos	488.2	3503	6.2	7.18
1990 OS	3.49	17.78	6.5	5.09
1999 RM45	5.12	38.28	13.5	7.48
2000 UG11	20.10	173.6	10.0	8.64
2002 AW	2.69	12.76	4.3	4.74
2002 TY57	5.01	44.16	10.3	8.81
2003 SS84	2.06	12.03	8.9	5.84
2003 UX34	22.44	168.2	11.5	7.50
2004 BL86	8.97	62.54	12.6	6.97
2006 GY2	9.97	92.50	11.1	9.28
2009 FD	7.46	69.19	8.6	9.27
2014 WZ120	35.21	253.3	14.5	7.19
2017 RV1	23.06	179.8	8.5	7.80
2018 TF3	4.61	41.64	11.9	9.03

Name	Primary diameter (m)	Secondary diameter (m)	Semi-major axis (m)	Period (days)
Didymos	780	170	1190	0.4971
1990 OS	300	50	600	0.875
1999 RM45	165	74	290	0.6852
2000 UG11	260	130	426	0.7667
2002 AW	230	50	520	1.047
2002 TY57	330	60	420	0.4485
2003 SS84	120	60	270	1
2003 UX34	280	100	460	0.625
2004 BL86	320	70	500	0.6
2006 GY2	400	80	500	0.487
2009 FD	150	90	250	0.6
2014 WZ120	300	100	500	0.56938
2017 RV1	300	100	470	0.5896
2018 TF3	270	60	350	0.438

Effects of Eccentricity

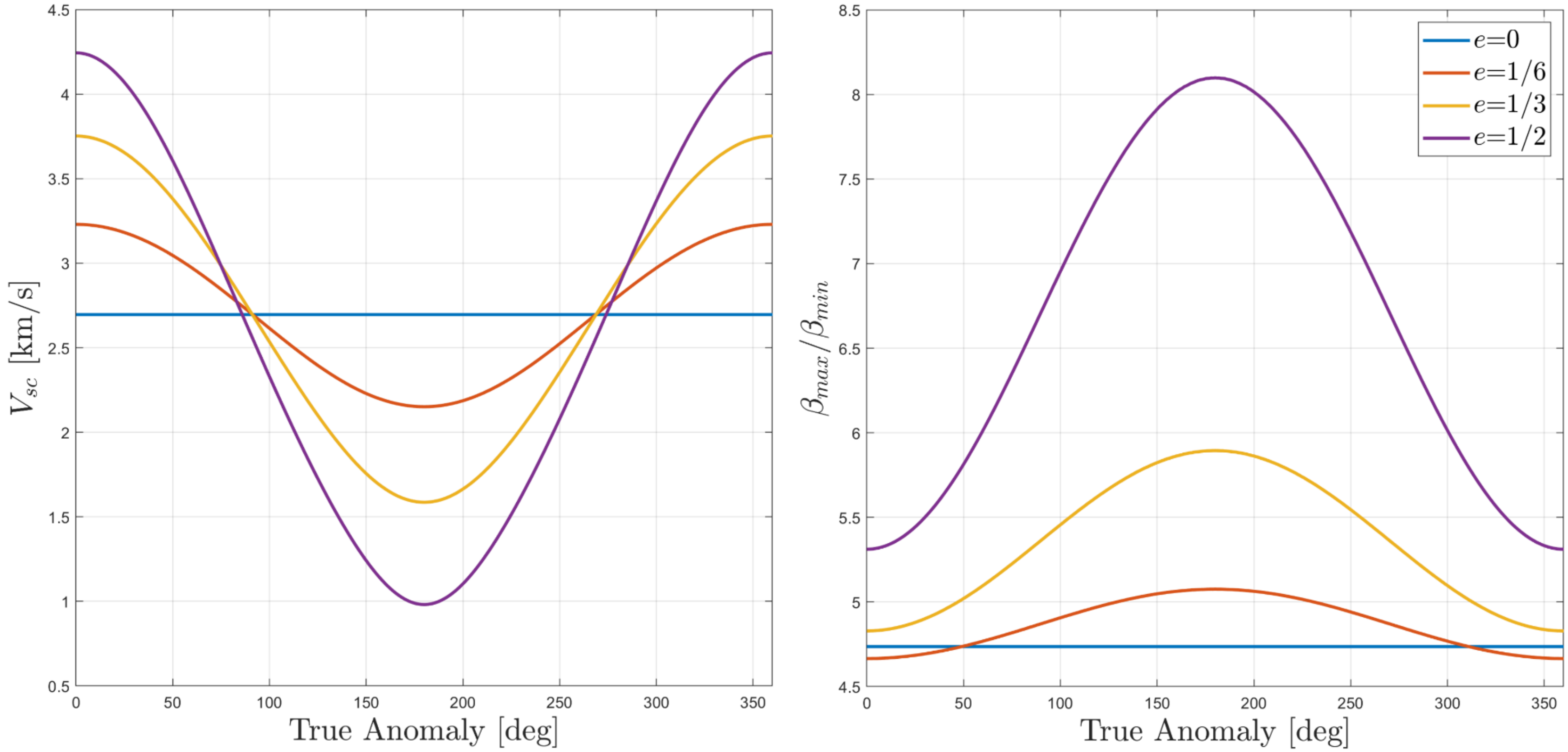

CR3BP

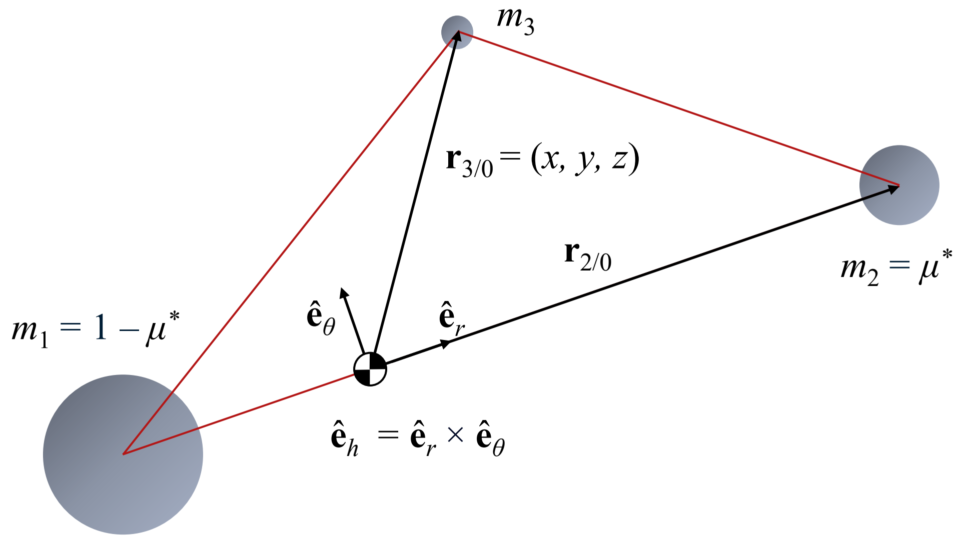
m_3
$\mathbf{r}_{3/0} = (x, y, z)$
$\mathbf{r}_{2/0}$
$m_2 = \mu^*$
$m_1 = 1 - \mu^*$
$\hat{\mathbf{e}}_\theta$
$\hat{\mathbf{e}}_r$
$\hat{\mathbf{e}}_h = \hat{\mathbf{e}}_r \times \hat{\mathbf{e}}_\theta$

Gauss

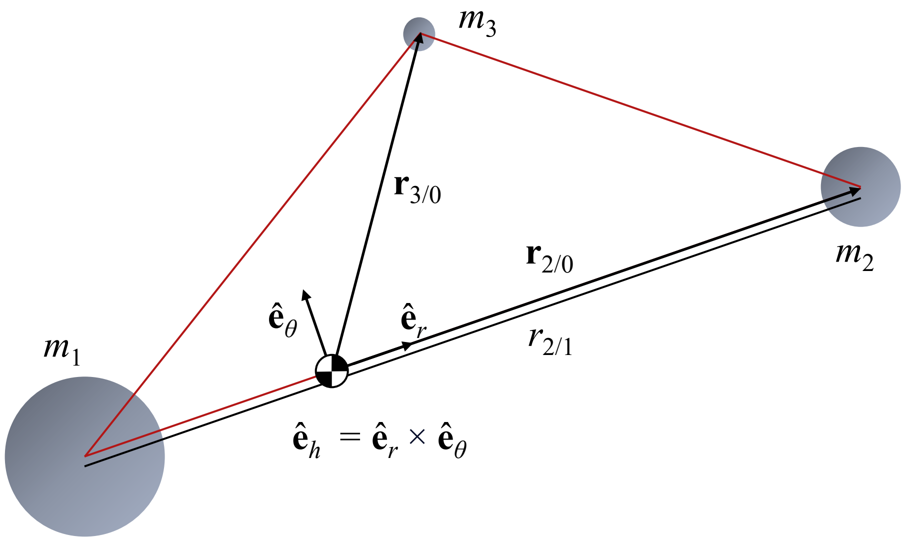
m_3
$\mathbf{r}_{3/0}$
$\mathbf{r}_{2/0}$
m_2
$\hat{\mathbf{e}}_\theta$
$\hat{\mathbf{e}}_r$
$r_{2/1}$
m_1
$\hat{\mathbf{e}}_h = \hat{\mathbf{e}}_r \times \hat{\mathbf{e}}_\theta$